Award Number: (W81XWH-12-1-0182

TITLE: Targeting the Prostate Cancer Microenvironment to Improve Therapeutic Outcomes

PRINCIPAL INVESTIGATOR: Yu Sun, Ph.D.

CONTRACTING ORGANIZATION: Seattle Institute for Biomedical and Clinical Research
Seattle, WA 98108-1532

REPORT DATE: August 2015

TYPE OF REPORT: Final

PREPARED FOR: U.S. Army Medical Research and Materiel Command
Fort Detrick, Maryland 21702-5012

DISTRIBUTION STATEMENT:

X Approved for public release; distribution unlimited

REPORT DOCUMENTATION PAGE

Form Approved
OMB No. 0704-0188

1. REPORT DATE *(DD-MM-YYYY)*	**2. REPORT TYPE**	**3. DATES COVERED** *(From - To)*
August 2015	Final	15 May/2012–15 May 2015

4. TITLE AND SUBTITLE

Targeting the Prostate Cancer Microenvironment to Improve Therapeutic Outcomes

5a. CONTRACT NUMBER
W81XWH-12-1-0182

5b. GRANT NUMBER
PC111703

5c. PROGRAM ELEMENT NUMBER

6. AUTHOR(S)
Yu Sun, Ph.D.

email: suny34@u.washington.edu

5d. PROJECT NUMBER

5e. TASK NUMBER

5f. WORK UNIT NUMBER

7. PERFORMING ORGANIZATION NAME(S) AND ADDRESS(ES)

Seattle Institute for Biomedical and Clinical Research
1660 S Columbian Way, S-151F
Seattle, WA 98108-1532

8. PERFORMING ORGANIZATION REPORT

9. SPONSORING / MONITORING AGENCY NAME(S) AND ADDRESS(ES)

U.S. Army Medical Research and Materiel Command
Fort Detrick, MD 21702-5012

10. SPONSOR/MONITOR'S ACRONYM(S)

11. SPONSOR/MONITOR'S REPORT NUMBER(S)

12. DISTRIBUTION / AVAILABILITY STATEMENT
Approved for public release; distribution unlimited.

13. SUPPLEMENTARY NOTES

14. ABSTRACT

Therapies designed to damage DNA (e.g. chemotherapy and irradiation) cure many primary prostate carcinomas (PCa) and produce significant responses in a subset of advanced malignancies. However, a subset of localized cancers resist genotoxic treatments, and most advanced cancers treated with such therapies eventually progress to a lethal phenotype. Thus, therapy resistance is a major contributor to PCa morbidity and mortality. We want to explore the hypothesis that DNA damaging therapeutics generates responses in benign cell types comprising the tumor microenvironment (TME) that promote tumor cell survival and enhance resistance. We have assessed the outcome of targeting individual mediators of this microenvironment-derived DDSP---specifically a member of the Wnt superfamily, WNT16B and demonstrated the highly effective neutralization of PCa cell malignancy *in vitro* by purified anti-WNT16B. We have established primary mouse prostate fibroblast cell lines and examined their responses including DDSP development upon DNA damage, and demonstrated the potential complication of regulatory mechanisms of DDSP program. Further, we determined the functional roles of the master regulators of DDSP including mTOR/NF-κB, and found the physical interaction between these molecules when cells are exposed to genotoxicity. We anticipate that targeting such a key signaling network is able to diminish treatment-initiated resistance conferred by the TME, and promote *in vivo* tumor responses in clinical settings of PCa medicine.

15. SUBJECT TERMS
Prostate cancer, microenvironment, DNA damage, genotoxicity, stroma, secretion, therapy resistance, outcome.

16. SECURITY CLASSIFICATION OF:			**17. LIMITATION OF ABSTRACT**	**18. NUMBER OF PAGES**	**19a. NAME OF RESPONSIBLE PERSON**
					USAMRMC
a. REPORT	**b. ABSTRACT**	**c. THIS PAGE**	UU	42	**19b. TELEPHONE NUMBER** *(include area code)*
U	U	U			

Standard Form 298 (Rev. 8-98)

Table of Contents

(Note: A request to terminate the award was made because of a recent institutional transfer of PI out of the country.)

INTRODUCTION

Contemporary therapies designed to target DNA (e.g. chemotherapy and radiation) cure many primary prostate carcinomas and produce significant responses in a subset of advanced metastatic cancers. However, a subset of localized solid tumors including prostate cancer resist genotoxic treatment, and most advanced malignancies treated with chemotherapy eventually progress to a lethal phenotype. Thus, therapy resistance is a major contributor to cancer morbidity and mortality. Several mechanisms responsible for resistance to genotoxic therapies have been identified and include the expression of drug efflux pumps, apoptotic deficiency, up-regulation of stress-responsive chaperone proteins, and enhanced mechanisms to repair mutations and DNA strand breaks. Though these mechanisms are clearly operative in a subset of tumors, *in vitro* studies of cancer cell lines poorly predict *in vivo* resistance, suggesting that cell autonomous and non-autonomous factors derived from the tumor microenvironment (TME) contribute to pro-survival effects.

A unique and robust secretory phenotype of prostate stromal cells as part of the response to DNA damage treatments was identified and termed a DNA Damage Secretory Program (DDSP). The DDSP complex is comprised of a large array of soluble factors known to influence tumor progression and includes proteases (MMP1/3/10/12), growth factors (HGF, AREG, EREG), pro-angiogenic factors (VEGF, ANGPTL4), and pro-inflammatory cytokines (IL6, IL7, IL8, IL1β). Components of the DDSP are also capable of promoting an epithelial to mesenchymal transition (EMT), a phenotype known to enhance resistance to cytotoxic and cytostatic cancer treatments. However, the underlying mechanisms that regulate such a cell non-autonomous secretory program remain largely unexplored, and their potential as novel therapeutic targets to be exploited for enhancing cancer sensitivity in clinical oncology has to be claimed.

BODY

We propose to test the concepts that (i) genotoxic treatment, in contrast to other cancer therapeutics, produces a robust paracrine-acting secretory program (DDSP) in benign components of the TME; (ii) specific components of the DDSP activate tumor cell survival signaling axes; and (iii) certain DDSP-activated programs (e.g. WNT signaling) can be exploited to enhance subsequent treatment responses. The following summarizes the technical objectives for the proposal and the work accomplished during the 1st year research period since the project initiation (05/15/2012 to date 06/14/2014, encompassing one year of interval as an intermittent period for institute transition from FHCRC to SIBCR).

Specific Aim 1: Determine the effect and effectiveness of inhibiting WNT16B, a key component of the prostate fibroblast DNA Damage Response Program, on prostate tumor responses to chemotherapy. Through these studies, this Aim will also assess the composition of the DDSP in specific cell types comprising the prostate TME and define damage responses produced by non-genotoxic agents.

Task 1.1: Establish xenografts compring PCa cells (PC3/VCaP) with PSC27 fibroblasts and examine tumor responses to single agent or combination therapy. (y 1/m 1-6)

1. Purification, refolding, and examination of human WNT16B antibody

First of all, we wish to study the feasibility and efficacy of anti-WNT16B antibody in down-regulation of prostate tumor progression in preclinical xenograft models. Our recent data demonstrated that components of the DNA damage response program produced by benign components of the tumor microenvironment contribute to enhanced tumor repopulation rates.

Particularly, the components of treatment-activated DNA damage secretory program (DDSP)—collectively or individually, alter neoplastric characteristics. One objective of the proposed work is to validate that key paracrine-acting molecules we have discovered, hereby exemplified by a *wingless-type MMTV integration site family member 16B*, WNT16B, as induced 33-fold upon DNA damage, are amenable to therapeutic targeting to enhance the effectiveness of commonly used prostate cancer therapies.

Extracellular drug targets have many advantages over intracellular ones, such as easy access by small-molecule inhibitors and antibodies. WNT16B is highly expressed in PCa patients post chemotherapy, and expression has been correlated with aggressive disease (Sun et al., 2012; Sun and Nelson, 2012). Our former work showed directly that WNT16B contributes to the aggressive phenotype, and forced expression of WNT16B increased PCa cell proliferation, mobility, invasiveness, and more remarkably, chemoresistance; in contrast, knockdown of this factor by genetic strategy significantly diminished tumor development. Thus, we plan to explore the hypothesis that the DNA-damaging regimen comprising a WNT16B-directed monoclonal antibody can result in decreased cancer malignancy, which allows improving PCa treatment through such an antibody-mediated administration. Together, future experimental findings may establish WNT16B as a new, specific, and -- by virtue of its outside-of-the-box location-- druggable target for the potentially lethal forms of prostate cancer.

To this end, it is essential to get purified anti-WNT16B as a first step. A solubilized mouse anti-human WNT16B monoclonal antibody from a commercial source prepared in aqueous buffered solution containing ≤0.09 % sodium azide, was purified by affinity chromatography using a Sephadex G25 gel filtration column. After one-step chromatographic purification in denaturing conditions, we optimized a cost saving dialysis procedure for correct refolding (Burgess 2009; Bel-Ochi et al., 2013) to improve the specific immunoreactivity of this complex molecule. The refolding procedure consists of consecutive dialysis baths with decreasing urea concentrations. The immunoreactivity recovery was confirmed by western blot analysis with whole cell lysates from PSC27 stable line that has been established by lentiviral infection to overexpress WNT16B (**Figure 1A**). No degradation products, protein aggregates or misfolded species were detected in the buffered antibody solution, as examined by anti-mouse HRP-conjugated secondary antibody (not shown). Typically, a 0.1 ml volume of 50 μg commercial raw antibody (Clone F4-1582) led to a final yield of about 40 μg purified anti-WNT16B. This amount even exceeded the terminal production estimated by the manufacture. Thus, our methodology allowed generation of anti-WNT16B that exhibit apparent biological activities and yielded sufficient products for downstream applications.

2. **Characterization of purified anti-WNT16B by delineating the influence of human prostate stroma damaged by genotoxicity on phenotypes of PCa epithelial cells**

To confirm the efficacy of anti-WNT16B generated through above procedures of purification and recovery, we applied the antibody to *in vitro* experiments. First, we looked at the influence of the antibody in affecting the proliferative augment gained by WNT16B as an overexpressed

soluble factor from the PSC27-WNT16B stable cell line. As compared with the buffer control, solutions containing purified anti-WNT16B significantly reduced the growth potential of BPH1, M12 and PC3 cells conferred by conditional media from stromal cells, although the effect to PC3 cells was most dramatic (**Figure 1B**).

As one of the prominent features of a full fibroblast DDSP program, conditional media from damaged fibroblasts upon ionizing radiation (PSC27-RAD) can stimulate the proliferation of neoplastic prostate cells. However, this tendency was significantly attenuated by antibody-mediated suppression (**Figure 1C**). Further, the enhanced invasive capacity of cancer epithelial cells by the full spectrum paracrine-acting fibroblast DDSP spurred by DNA damaging treatment (PSC27-RAD), was remarkably suppressed by purified anti-WNT16B (**Figure 1D**).

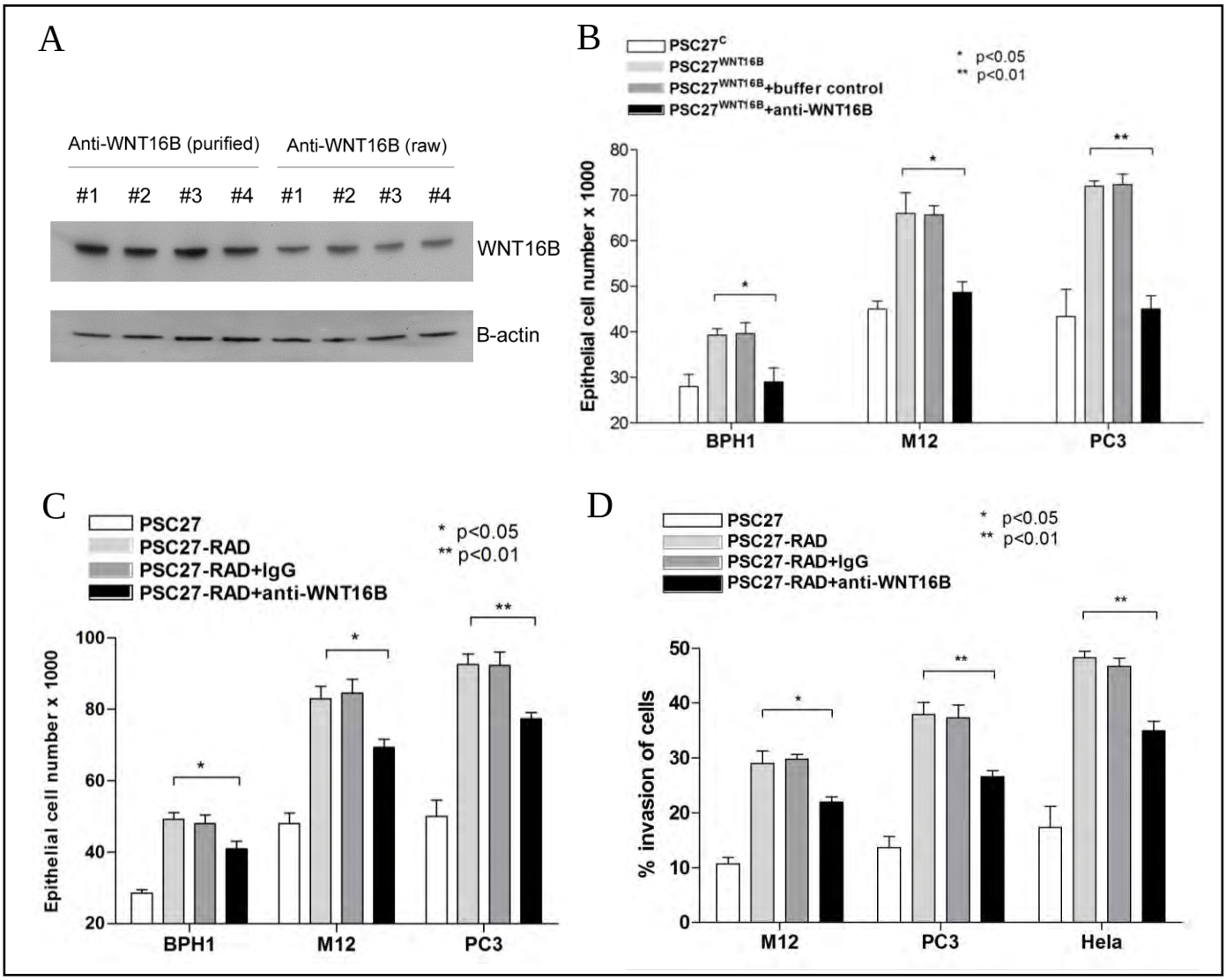

3. Establishment of xenografts comprising PCa (PC3/VCaP) implanted with PSC27 and examination of tumor responses to single agent or combination therapy

We have built xenografts comprised of PC3 or VCaP cells with PSC27 fibroblasts, and allowed the tumors to reach 300 mm^3 prior to chemical treatments. The tumor-bearing animals were assigned to four groups: Group 1 (control, IgG/Placebo), Group 2 (IgG/0.2 mg/kg MIT i.p. q week), Group 3 (anti-WNT16B antibody 500 µl, at 10 mg/kg body weight/Placebo 2x weekly), Group 4 (0.2 mg/kg MIT i.p q week with anti-WNT16B antibody 10 mg/kg body weight 2x weekly). The effectiveness of single agent or combination therapy was determined by assessing immediate tumor responses 3 days after the first MIT dose, including tissue staining for (1) β-catenin to analyze anti-WNT16B activity, (2) caspase 3 to assess response to cytotoxicity; and tumor volumes measured 2 weeks after 3 MIT cycles.

Upon preliminary examination of xenograft sections derived from these animals, we found that within 3 days of immunotherapy the basal protein level of β-catenin throughout the cells decreased once anti-WNT16B was administered. More importantly, the nuclear translocation of β-catenin in mice treated with MIT, a type II topoisomerase inhibitor that disrupts DNA synthesis and DNA repair, was substantially inhibited by anti-WNT16B (**Figure 2A**). To further determine acute responses of tumors after the first dose of MIT treatment, we examined caspase 3, a typical cysteine-aspartic acid protease activated during apoptosis by extrinsic (death ligand) or intrinsic (mitochondrial) pathways. Our data indicated that caspase 3 levels in placebo-group did not change very much by anti-WNT16B, however, its levels in the MIT-group significantly increased once anti-WNT16B was applied (**Figure 2B**). To profile the difference, we compared the percentage of caspase 3-intensive cells in each individual area of tissues examined (**Figure 2C**). Similarly, xenograft composed of VCaP cells and PSC27 fibroblasts demonstrated the efficacy of anti-WNT16B in promoting chemosensitivity under *in vivo* conditions (**Figure 2D**).

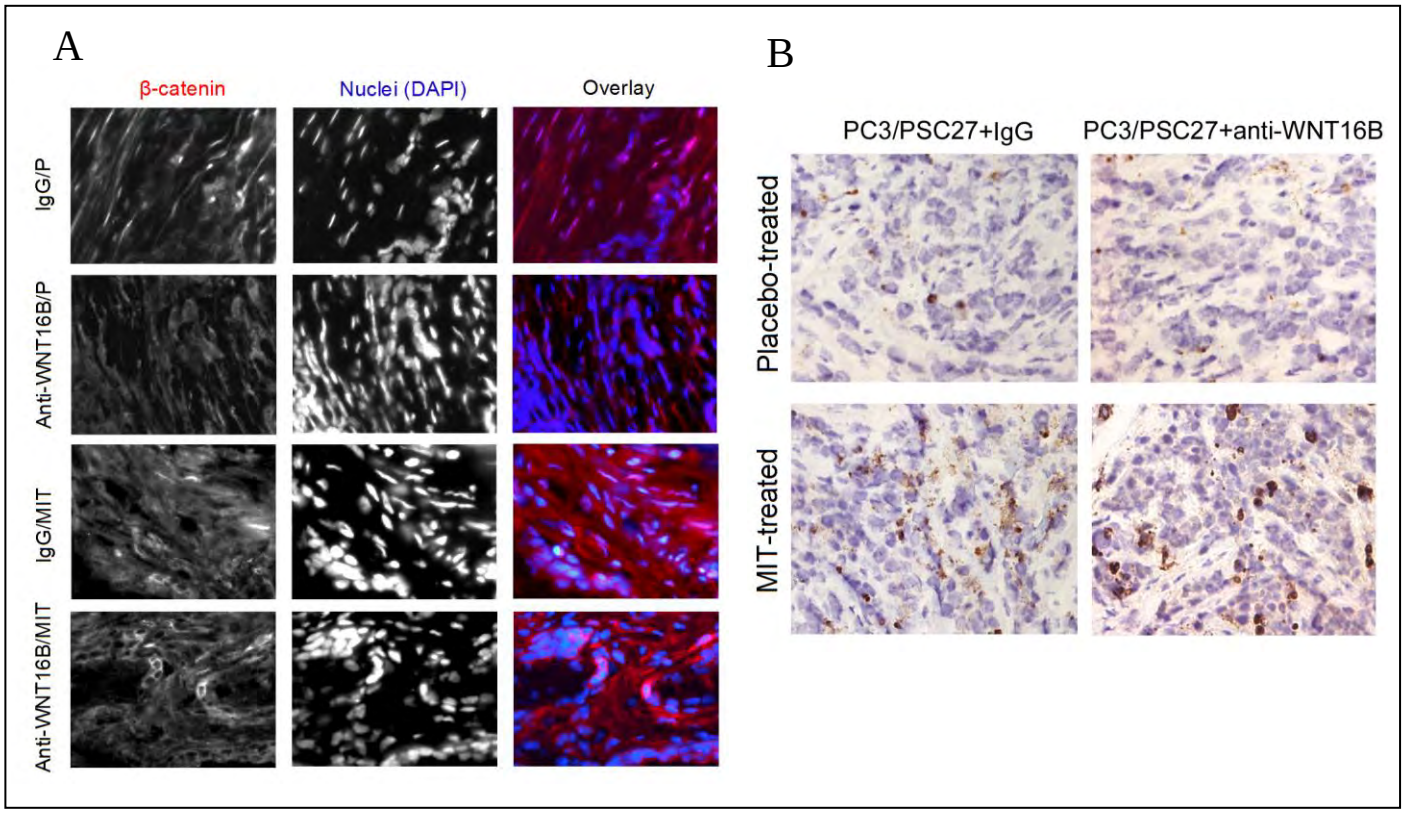

C

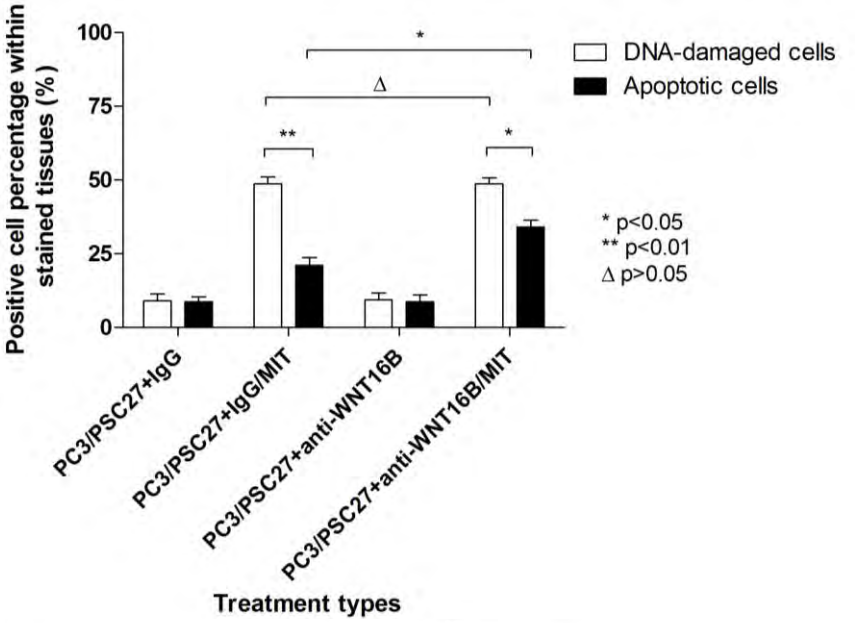
Positive cell percentage within stained tissues (%)
100
75
50
25
0
*
Δ
**
*
DNA-damaged cells
Apoptotic cells
* p<0.05
** p<0.01
Δ p>0.05
PC3/PSC27+IgG
PC3/PSC27+IgG/MIT
PC3/PSC27+anti-WNT16B
PC3/PSC27+anti-WNT16B/MIT
Treatment types

D

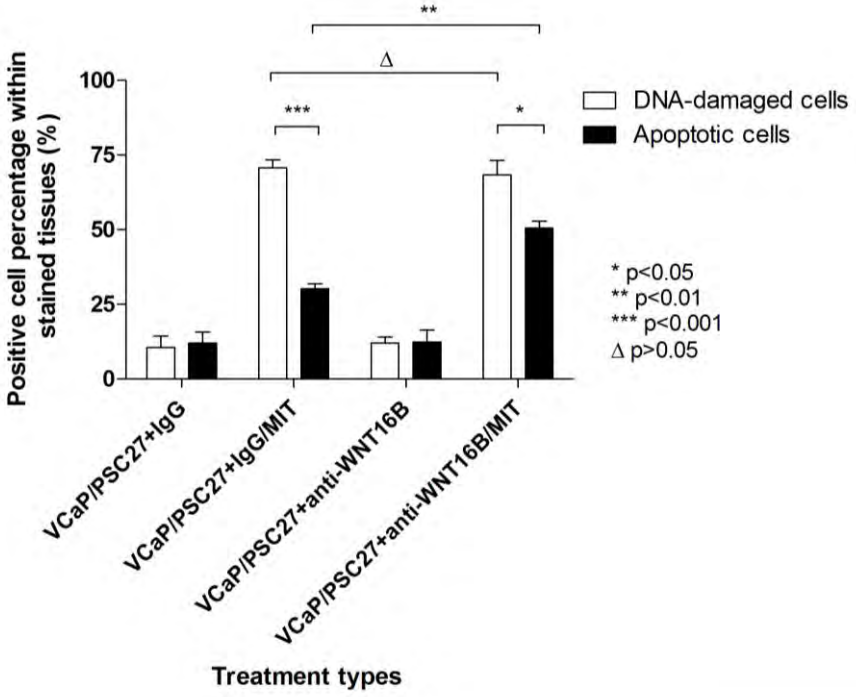
Positive cell percentage within stained tissues (%)
100
75
50
25
0
**
Δ
***
*
DNA-damaged cells
Apoptotic cells
* p<0.05
** p<0.01
*** p<0.001
Δ p>0.05
VCaP/PSC27+IgG
VCaP/PSC27+IgG/MIT
VCaP/PSC27+anti-WNT16B
VCaP/PSC27+anti-WNT16B/MIT
Treatment types

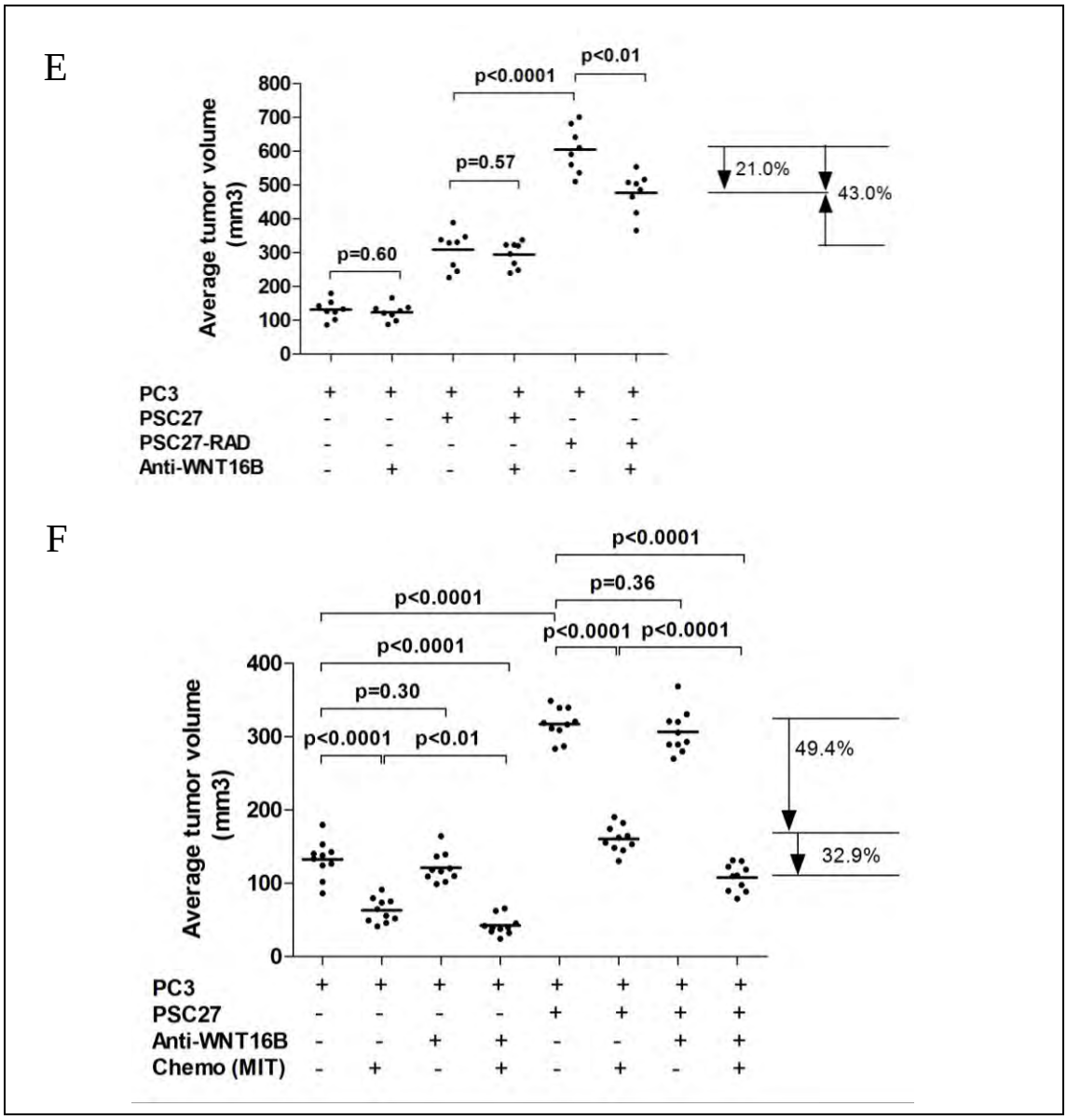

Figure 2. Establishment and examination of xenografts comprising prostate cancer epithelial cells (PC3 or VCaP) and PSC27 fibroblasts, and of tumor responses to immuno- and/or chemotherapy

A. Immunofluorescence staining of β-catenin on tissue sections from mouse xenografts made of a mixture of PC3 (or VCaP cells) and PSC27 fibroblasts (1:1 ratio upon implantation). Secondary antibody conjugated with Alex 594 was used to probe primary antibody against β-catenin (monoclonal), while DAPI was used to stain nuclei. **B.** Immunohistochemistry staining with anti-caspase 3 on these tissue sections. **C** and **D.** Statistics of percentage of cells (in PC3 and VCaP tumors, respectively) stained acutely positive for caspase 3 on xenograft sections of mice upon therapies. **E** and **F**. End point measurement of the 8 week growth of tumors consisting of PC3 and PSC27 as xenografts implanted together to subcutaneous cavity, chemotherapy and/or immunotherapy was performed during the period. Suppression with the WNT16B-specific antibody enhanced the response of tumor xenografts to mitoxantrone-based chemotherapy regimen.

Task 1.2: Determine the role(s) of inflammatory cell responses in the TME with immune-competent mouse models. (y 1/m 7-12)

In this study, the type of animals will be Pb-Myc mouse model (FVB background) that was established ~ a decade ago by Dr. Charles Sawyers at UCLA, as a pilot transgenic tool for PCa research community. Under this arm, no cell lines will be used for the experiments. Due to the recently met difficulty in acquiring enough mice that are Pb-Myc transgene positive and able to develop palpable tumors at the designated time point in their lifetime, we are managing to get sufficient data so far. No figures available at this moment.

Task 1.3: Develop a system for studying signal transduction programs and other components of the TME regulated by WNT16B in the context of an intact immune response. (y 2/m 1-6)

Establishment and characterization of primary prostate fibroblast lines from the FVB mouse strain

To examine the effects of WNT16B on tumor growth and therapy resistance, and clarify signal transduction programs and other components of the tumor microenvironment (TME) regulated by WNT16B in an intact immune system, primary mouse prostate stromal cells particularly fibroblasts are highly desired as they can serve as a baseline for future tissue recombination experiments. This will allow replication of renal capsule xenograft studies (EXP1) that comprises recombined cell types, substituting Myc-CaP (Watson et al., 2005) mouse prostate cancer cell lines and corresponding mouse fibroblasts engineered to overexpress or suppress WNT16B in the context of mitoxantrone (MIT) therapy. Myc-CaP cells will allow for grafting in syngeneic *immune-intact* mouse hosts (e.g. FVB for Myc-CaP) to assess for possible immune regulatory influences of WNT16B in the TME that could enhance, or suppress WNT16B tumor effects.

For this purpose, we derived primary mouse prostate fibroblasts from wild type FVB mice at the age of 3~4 months (puberty). Nutrient specificity, morphology and growth pattern of these primary fibroblasts were characterized. For optimization of the mouse fibroblasts (MFs) culture, we tested several conditions such as DMEM versus DMEM/F12, F-10 Nutrient Mixture, Ham's F12 Nutrient Mixture, α-MEM with or without bFGF and StemXVivo medium (Sung et al., 2008; Futami et al., 2012). When the MFs were maintained with enriched culture media, such as DMEM/F12 or α-MEM with or without bFGF, cell proliferation was inadequate and cell morphology changed to flat, enlarged shapes (data not shown). However, with the routine DMEM medium the results improved with an adequate volume of cells and normal morphology. It is noteworthy that the initial culture of the isolated MFs had a heterogeneous cell population with both round and spindle (fibroblastic) cells. However, the number of round-shaped cells gradually decreased and the growth rate of the fibroblastic cells increased over time upon sequential subculture. Generally, the MFs isolated from the prostate tissues of FVB mouse strain showed fibroblastic morphology (**Figure 3**). The morphologic characteristics of the MFs were similar to NIH3T3, an established mouse embryonic fibroblast line from ATCC. However, the average growth rates of the MFs were even higher. In addition, colony-forming unit fibroblast (CFU-F) numbers were used to compare various growth potentials among the fibroblasts from different sources (Sung et al., 2008). To estimate the CFU-F number, 1000 cells were plated onto a 100-cm^2 dish, and then cultured for 7 days. One subline of MFs, F4M3 showed the highest

number of CFU-Fs (**Figure 4A**). Therefore, our results suggest that F4M3 is a mouse fibroblast line that can be potentially suitable for *in vitro* studies of cell biology and *in vivo* experiments of tumor implantation.

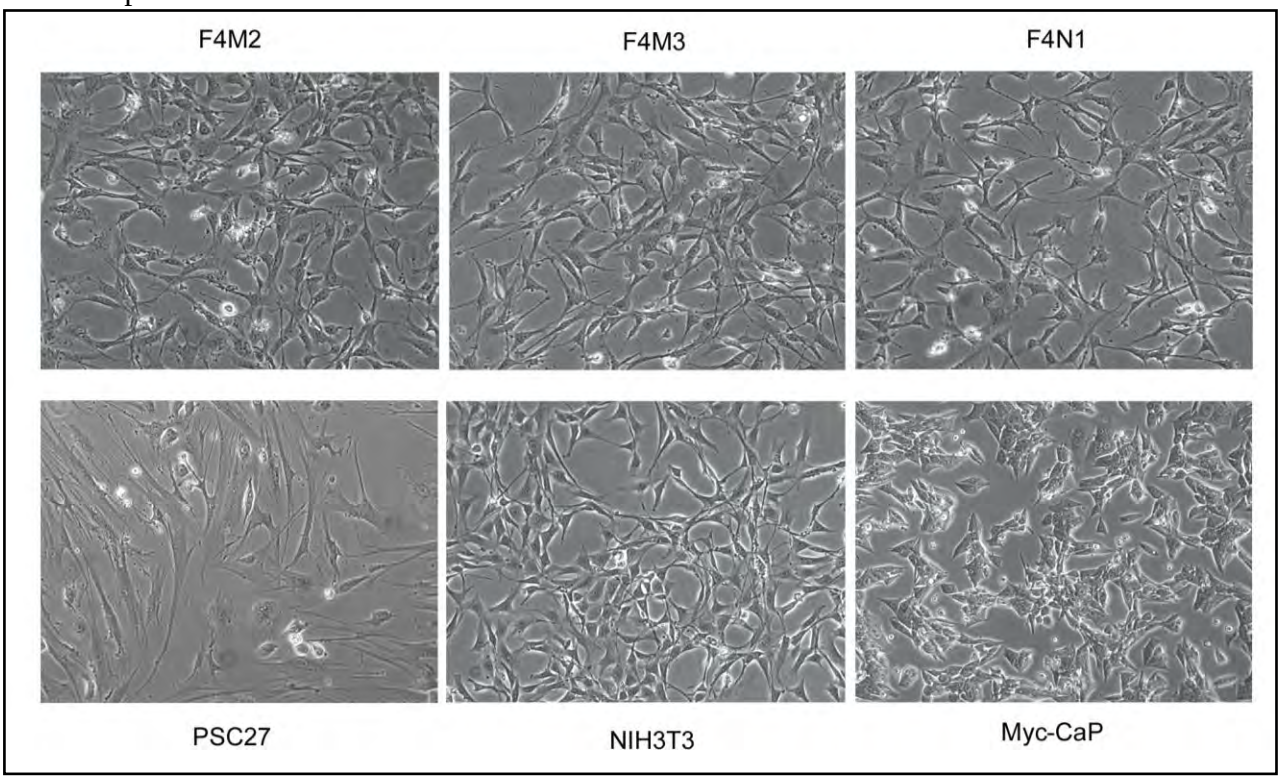

Figure 3. Cell morphology of primary prostate fibroblast lines isolated from FVB mice. Bright field microscopic images of 3 representatives of such cell lines are shown, and cells are maintained in optimized culture media. Among them, F4M3 grows faster than others, and all three lines resemble NIH3T3, a well-established and widely used mouse embryonic fibroblast line. The primary normal human prostate stromal line PSC27, and Myc-CaP line originally derived from High-Myc transgenic mouse model of prostate cancer, both cultured in DMEM/10%FBS, serve as parallel controls.

For molecular identification of these cell lines, whole cell lysates were collected from culture and applied for immunoblot analysis. Interestingly, the fibroblast-specific markers, including vimentin and α-SM actin were consistently expressed in the established lines, with F4M3 examined as a representative, while the typical luminal epithelial markers mainly E-cadherin and CK8 are basically missing (**Figure 4B**). This is in line with NIH3T3 cells, which is well known for its fibroblast feature, although from a different mouse strain. Thus, the expression profile of our primary mouse prostate fibroblasts is confirmed, which appears unique and distinct from the well-established mouse prostate cancer cells of the same genetic origin (FVB).

In addition, we determined the response of F4M3 cells upon ionizing radiation. Not surprisingly, multiple secreted factors as hallmark of typical DDSP phenotype that was reported in human fibroblasts were markedly enhanced within 10 days post DNA damage (**Figure 4C**). However, the expression of a few soluble factors, particularly SPINK1, CXCL14 and CCL26 remained largely unchanged, when the mTOR suppressor RAD001 was applied to the culture conditions.

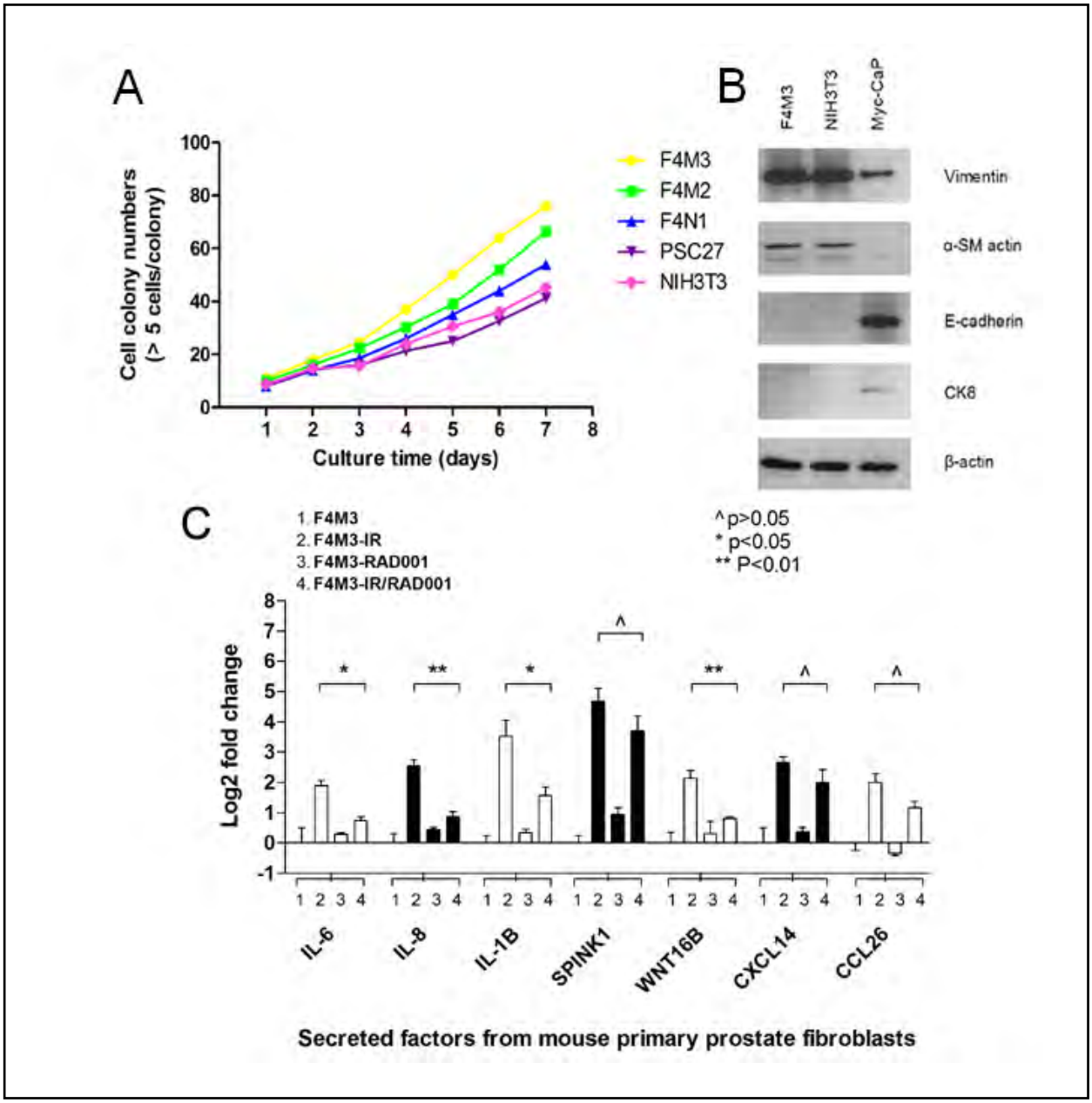

Thus, even in the presence of a small molecule inhibitor of DDSP, part of the whole spectrum of secretion is unaffected, indicating the complexity of such a fibroblast-specific program and the necessity to thoroughly explore the multiple mechanisms of DDSP development, some of which are so far still cryptic and unclear.

Figure 4. Growth potential and expression pattern of cell line specific markers. **A.** Colony-forming unit (CFU) is counted for cell lines cultured under the optimized conditions, in a consecutive 7-day period. To estimate the CFU number (>5 cells/colony), 1000 cells are plated onto a 100-cm^2 dish, with media changed every 2~3 days. One subline of MFs, F4M3 exhibited the highest number of CFUs. **B.** Western blots of cell lines with antibodies against several cell lineage specific markers applied. Actin, loading control for signal normalization. **C.** Expression of several typical DDSP factors in F4M3 line upon DNA damage, which was differentially altered by a small molecule drug, RAD001. Note, the expression of SPINK1, CXCL14 and CCL26 promoted by genotoxicity, cannot be completely blocked upon RAD001 treatment, making them unique among multiple DDSP factors.

Task 1.4: Determine the tissue and cell type-specific consistency and variation of DDSP response. (y 1/m 7-12)

The aims of this arm are to assess for the effects of: i) genotoxic chemotherapy; ii) the full fibroblast-derived DDSP, and iii) specifically WNT16B, on the immune cell composition in the TME. We would resect prostate tumors (complete prostate glands) as well as tissues commonly harboring prostate cancer metastasis (e.g. lymph node, bone) in a replicate experiment corresponding to EXP2 of the proposal. After 3 cycles of therapy (4 treatment arms), tumors and organs will be resected. However, due to the same reason as described in Task 1.2, we have not been able to go very far for these experiments, and will focus on the scheduled research activities once enough mice are collected in the next stage.

Task 1.5: Characterize the uniqueness and extent of DDSP generated upon DNA damage as compared to alternative mechanisms (non-genotoxic). (y 1/m 7-12)

To do this, we tested the influence of several chemical agents that are commonly used in the settings of clinical oncology. According to the practical purposes of these agents, we organized them into two groups, namely DNA-targeting and none DNA-targeting. The former included bleomycin (BLEO), mitoxantrone (MIT) and ionizing radiation (RAD), while the latter covered docetaxel, paclitaxel and vincristine. Each of these chemicals was tested in a preliminary study to determine an appropriate concentration so that PSC27 fibroblasts were subject to induction of senescence but not apoptosis under *in vitro* culture conditions. Interestingly, although non-genotoxic chemicals changed cell morphology in a manner that was distinct from genotoxic agents, there was not much difference in the staining pattern by β-Gal between these two classes (**Figure 5A, B**). We examined the extent of DNA damage and results were basically in line with the original speculation (**Figure 5C)**. Intriguingly, we found the mitogen-activated protein kinase (MAPK) p38, a signaling protein activated by a variety of environmental stresses and inflammatory cytokines, became rapidly phosphorylated by all of these treatments. Further, p38 was involved in regulation of the small molecular chaperone HSP27 upon such a series of cell

stress (**Figure 5D**). We interrogated whether the secretion phenotype of PSC27 fibroblasts was developed as part of the downstream cellular reactions, and the results indicated a consistently emerging but differential DDSP program under all of these stress conditions (**Figure 5E**). Thus, it is quite tempting to investigate the underlying mechanism that led to the activation of a pivotal network and cascade formation of prostate stromal secretion upon genotoxic stress.

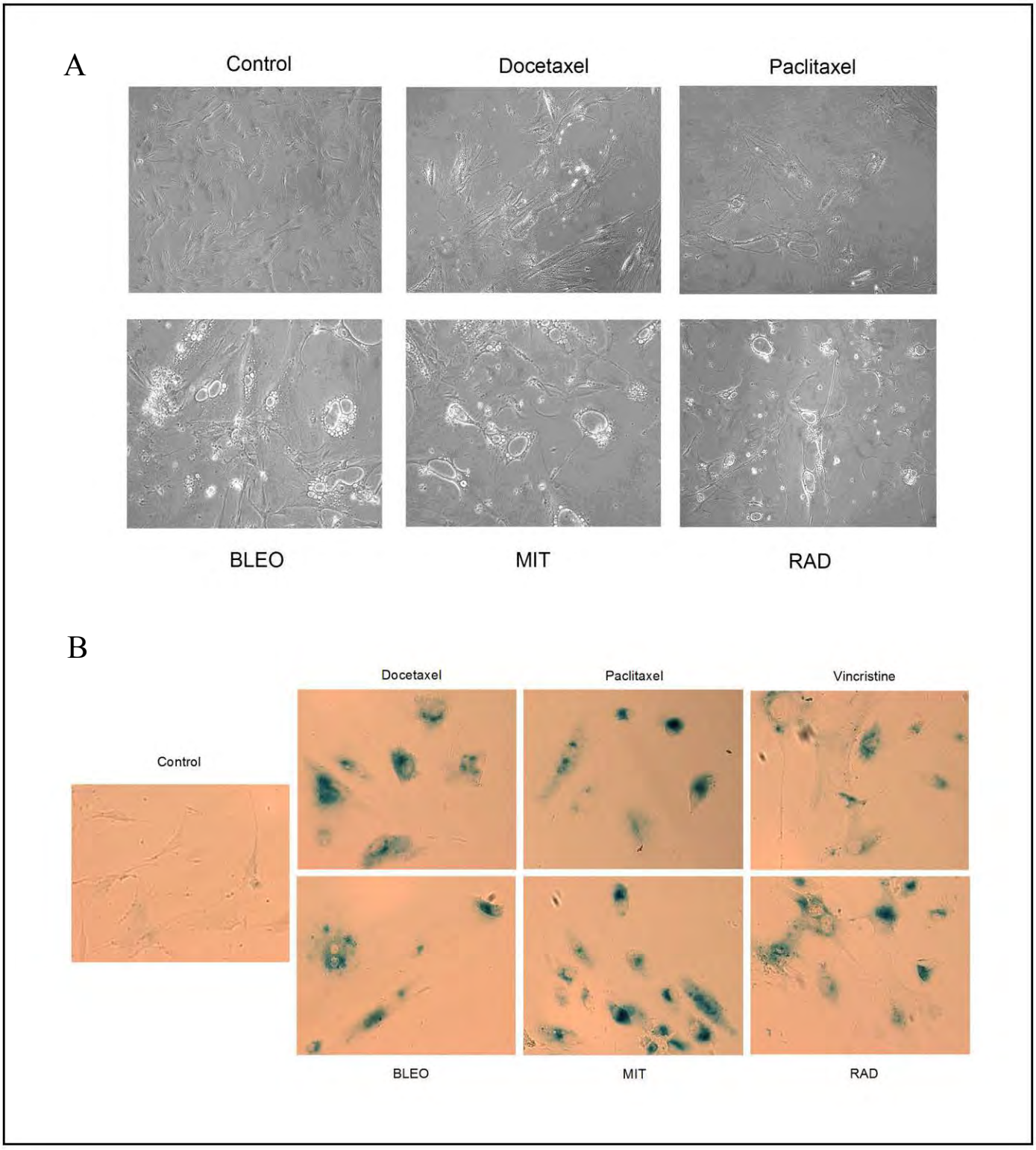

C

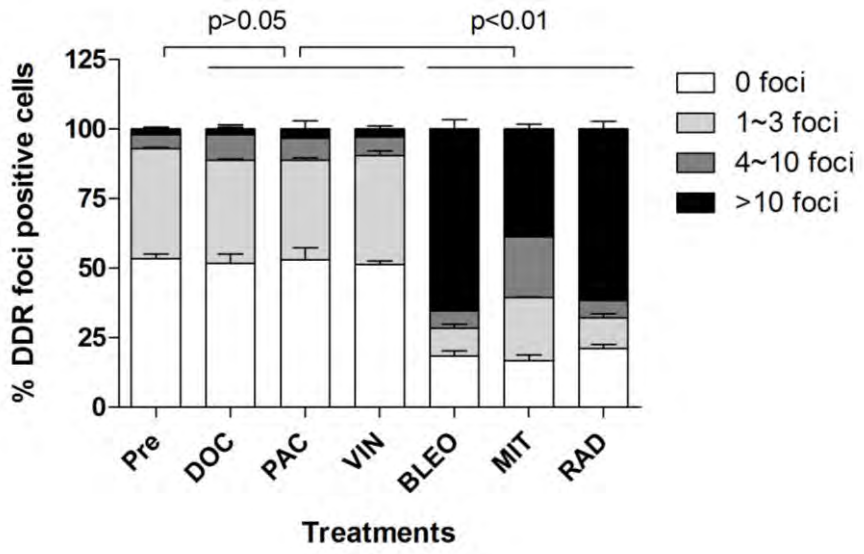
p>0.05
p<0.01
% DDR foci positive cells
125
100
75
50
25
0
0 foci
1~3 foci
4~10 foci
>10 foci
Pre
DOC
PAC
VIN
BLEO
MIT
RAD
Treatments

D

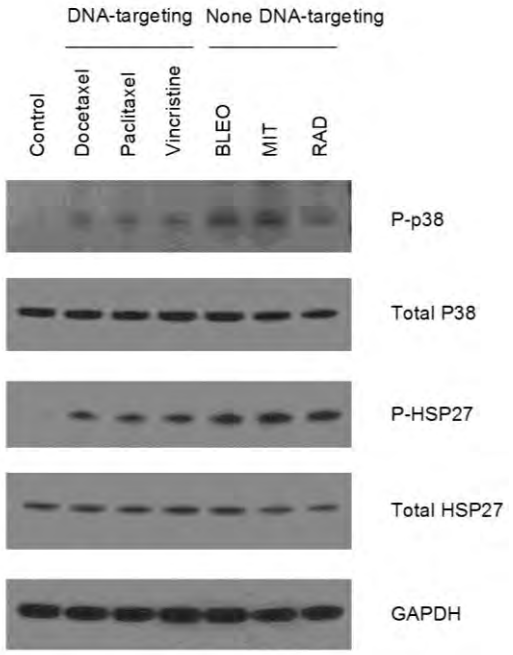
DNA-targeting
None DNA-targeting
Control
Docetaxel
Paclitaxel
Vincristine
BLEO
MIT
RAD
P-p38
Total P38
P-HSP27
Total HSP27
GAPDH

E

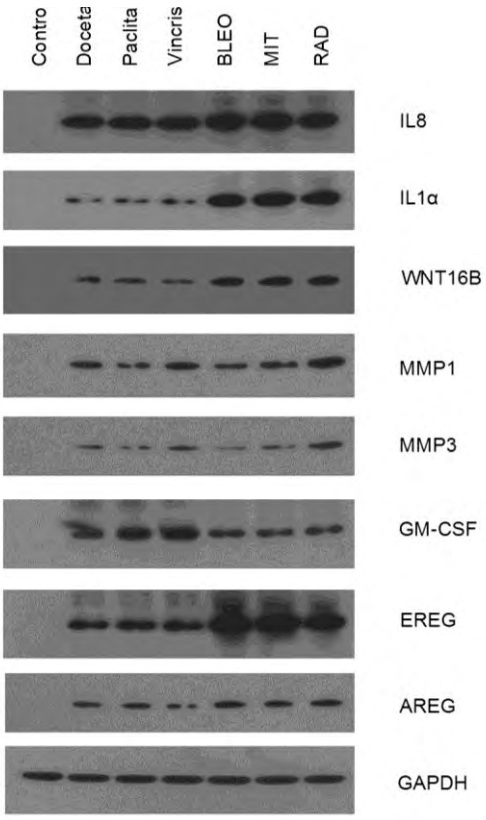
Contro
Doceta
Paclita
Vincris
BLEO
MIT
RAD
IL8
IL1α
WNT16B
MMP1
MMP3
GM-CSF
EREG
AREG
GAPDH

F

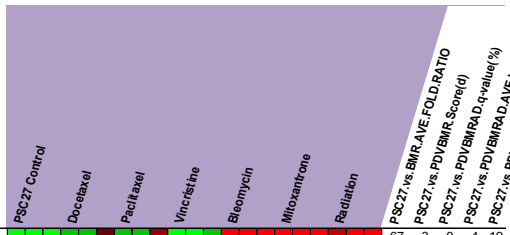

GeneSymbol	PSC27.vs.BMR.AVE.FOLD.RATIO	PSC27.vs.PDVBMR.Score(d)	PSC27.vs.PDVBMRAD.q-value(%)	PSC27.vs.PDVBMRAD.AVE.LOG2.RATIO	PSC27.vs.PDVBMR.AVE.FOLD.RATIO
SPINK1	67	3	0	4	19
ESM1	18	2	0	2	5
TNFSF15	18	5	0	3	10
SERPINB2	14	4	0	3	7
SPINK13	14	3	0	3	6
CGA	13	3	0	3	7
SPP1	13	2	0	2	4
TAC1	13	2	0	2	5
IL24	12	5	0	3	9
NTS	10	1	2	2	3
CCL3	9	5	0	3	6
COL10A1	9	2	0	2	4
LIPF	8	2	1	2	3
GPC5	8	2	1	2	3
PNLIP	8	1	2	1	3
NPTX2	7	2	0	2	3
CA2	7	2	1	1	3
SPARCL1	7	1	2	1	3
CA6	7	1	3	1	3
LYZL2	6	1	2	1	3
IL1RL1	6	4	0	2	5
FGF12	6	2	1	1	3
FREM3	6	2	0	2	3
SFRP2	6	3	0	2	4
SCGB2A1	6	2	2	1	2
FGF16	6	2	0	1	3
SPINK4	5	2	0	2	3
FGF18	5	3	0	2	3
CALCA	5	2	1	1	2
CCL3L3	5	5	0	2	4
CCL20	5	3	0	2	5
CLCA2	5	7	0	2	5
PPBP	5	3	0	2	4
C4orf7	5	3	0	2	3
NPPC	5	1	4	1	2
HS3ST4	5	2	0	1	2
HBEGF	5	3	0	2	3
GKN1	5	3	0	2	3
PRG4	5	1	3	1	2
CSF2	5	5	0	2	4
ANGPT2	5	2	0	1	3
EPGN	5	2	1	1	2
MUCL1	5	2	0	2	3
AMY1C	5	4	0	2	3
SCG2	5	3	0	2	3
CCK	5	4	0	2	4
MFI2	5	2	0	1	2
GDF15	5	4	0	2	3
GABRB1	5	2	0	1	2
SPINK2	5	2	0	1	2
LYZL1	5	1	2	1	2
NELL2	5	1	2	1	2
CXADR	5	4	0	2	3
APOH	5	1	2	1	2
CPB2	4	1	4	1	2
C4orf26	4	1	2	1	2
LIPG	4	1	7	1	2
FOLR3	4	2	0	1	2
EMCN	4	1	3	1	2
LY96	4	2	0	1	2
SFRP4	4	2	0	1	2
SERPIND1	4	2	0	1	3
CCL18	4	4	0	2	3
CPE	4	2	0	1	3
IL8	4	5	0	2	4
CDKN2B	4	4	0	2	3
FSTL5	4	2	1	1	2
HAPLN1	4	2	0	1	2
IL1B	4	3	0	2	5
IL23A	4	3	0	2	4
SCRG1	4	2	0	1	3
LPA	4	1	4	1	2
GCG	4	2	1	1	2
FST	4	2	0	1	3
PMCH	4	1	2	1	2
TF	4	2	0	1	2
GKN2	4	1	4	1	2
CRH	4	2	1	1	2
OTOL1	4	1	2	1	2
LIF	4	4	0	2	3
ALB	4	3	0	1	3
DEFB1	4	1	2	1	2
BMP7	4	2	0	1	2
PNOC	4	1	2	1	2
SCG3	4	2	1	1	2
MMP10	4	1	7	1	2
MSMB	4	1	4	1	2
PRL	4	2	0	1	3
SMOC2	4	2	2	1	2
OTOA	4	2	2	1	2
IFI27	4	3	0	1	3
TMEFF2	4	1	2	1	2
TNFSF4	4	3	0	1	3
INSL4	4	1	3	1	2
AMBN	4	1	4	1	2
GABRA2	4	2	0	1	2
CRHBP	3	2	2	1	2
NELL1	3	1	8	1	2
TTR	3	1	2	1	2
ITLN1	3	1	3	1	2

Figure 5. Characterization of the uniqueness and extent of stromal DDSP upon DNA damage by applying drugs that engage alternative targeting mechanisms (genotoxic vs non-genotoxic). **A.** Phase contrast images of PSC27 cells under various conditions. **B.** β-Gal staining profiles of cells post treatment, images were taken 12hr after cell-in-well incubation at 37℃. **C.** Senescence-associated damage foci (SADF) in PSC27 cells in response to chemo agents. **D.** Immunoblot analysis with lysates collected from PSC27 cells that were subject to 3 microtubule toxins and 3 DNA damaging agents, respectively, with p38 and HSP27 as major cytoplasmic objectives. **E.** Immunoblot of several hallmark DDSP factors including IL8, IL1α, WNT16B, MMP1, MMP3, GM-CSF, EREG and AREG. Each case, conditioned media and cytosol of PSC27 cells were collected, and subject to parallel analysis. **F.** Expression heapmap at transcript level of top 100 extracellular factors synthesized by damaged stromal cells upon above treatments.

Specific Aim 2: Identify key upstream 'master regulators' of the DNA Damage Secretory Program and assess the anti-tumor effects of broad DDSP suppression. Through these studies the effects of the composite DDSP will be defined using 3D assays of cytotoxicity and preclinical model systems.

Task 2.1: Demonstrate the influence of damaged TME cells through *in vitro* cell culture assays.

Select cells and treatments to initiate damage response (y 2/m 1-6)

We compared several human prostate cell types including cancer epithelial lines (PC3, DU145, VCaP, LNCaP and CWR22RV1), benign epithelial lines (wrBPH1, RWPE1/2) and fibroblast lines (PSC27, PSC31, PSC36), in terms of cellular responses to DNA damage. We determined that PSC27 stands an ideal stromal line that is capable of demonstrating typical DNA damage repair activities, subsequent pathway/network activation and ensuing development of robust secretory phenotype (not shown).

Modulate the pathways of potentially critical mediators of DDSP response (y 2/m 1-6)

Demonstrate the influence of DDSP master regulators in mediating adverse carcinoma phenotypes through paracrine effects of the TME (y 2/m 7-12)

While tumor resistance is established as a consequence of intrinsic genetic and epigenetic changes of cancer cells, emerging evidence indicates that the DNA damage secretory program (DDSP) resulting from genotoxic therapeutics confers acquired insensitivity to subsequent treatments. The mammalian target of rapamycin (mTOR) kinase is a master regulator of cellular responses to multiple stimuli including nutrient stimulation and adverse insults; however, the molecular link to its downstream regulatory nodes of gene expression correlated with DDSP is elusive. In this study, we show that genetic or chemical inhibition of mTOR suppresses DDSP phenotype. We identified a physical association between mTOR and the I-kappa-B kinase (IKK) complex upon cellular exposure to DNA damage agents, an event causing the central action-p65/p50 nuclear translocation. Formation of mTOR/Raptor complex is activated by genotoxic stress and promotes NF-κB signaling, and paracrine-acting DDSP factors are regulated through both transcriptional and post-transcriptional mechanisms. We determined that mTORC1 is the

predominant mediator of the DDSP development, and it receives signals from upstream kinases including the PI3K/Akt node. Our studies establish mTOR as a novel target for therapeutic intervention to abrogate mechanisms of resistance derived from the tumor microenvironment (TME) upon genotoxicity, and suggest that mTOR inhibitors may be repurposed to sensitize cancer cells to DNA-damaging therapeutics.

Identification of mTOR as a crucial mediator of DDSP phenotype in response to genotoxic stress

First, we asked if rapamycin attenuates DNA damage signals and converts an irreversible senescent growth arrest into a reversible quiescent arrest, as reported for certain transformed cells (Demidenko et al., 2009). However, we found this was not the case for normal prostate fibroblasts. PSC27 cells harbor persistent γH2AX foci upon senescence caused by ionizing radiation (IR) (**Figures 6A and 6B**), oxidative stress (H_2O_2) or Mitoxantrone (MIT) treatment (not shown), but these foci were unaltered by rapamycin. Likewise, rapamycin failed to abrogate the senescent grow arrest, as determined by cell population doubling (counting) and cell cycle arrest (BrdU incorporation) assays (**Figures 6C and 6D**). However, the percentage of SA-βgal positive cells decreased 43% when rapamycin was applied to the culture conditions (**Figures 6E)**, indicating consistently suspended proliferation but reduced metabolic rate of damaged cells, in contrast to conditions without rapamycin.

Importantly, we looked at the nuclear translocation and activity of NF-κB as a major stress, inflammation, cell survival and organism homeostasis regulator in eukaryotes. At a modest concentration of 15 nM in culture conditions, rapamycin was able to remarkably inhibit nuclear translocation and transcriptional activity of NF-κB under genotoxic *in vitro* conditions generated by IR (**Figure 7A**).

Based on the fact that significant changes of multiple soluble factors secreted from stromal cells can be caused by DNA damage, we applied rapamycin to cells that were subsequently exposed to IR. As compared with the regular treatment results, upregulation of most of the DDSP hallmarks was dramatically attenuated or even abolished, with their fold change limited to a minimal level as indicated by the transcription signals (**Figure 7B**). In addition, a large array of such DDSP-associated factors was among those genes with overexpression remarkably reduced upon DNA damage (not shown).

To examine the influence of such suppressed development of stromal DDSP on cancer cell progression, we measured the ability of fibroblast-derived conditioned media (CM) to stimulate epithelial growth. PSC27 cells were cultured with rapamycin when radiated, and incubated for 10 days to allow development of a typical DDSP phenotype before CM collection, which was subsequently applied to epithelial cells. Interestingly, the growth potential was comprehensively compromised in all the lines tested (**Figure 7C**). It has been reported that CM generated from damaged fibroblasts can enhance the migration and invasion of cancer epithelial cells across matrix-coated membrane; however, such capabilities of CM made from damaged cells in the presence of rapamycin were dramatically diminished (**Figures 7D and 7E**).

Moreover, by testing the potential of a large body of DDSP factors in protecting epithelial cells against cytotoxicity of pharmacological agents, we noticed the reduced gain of survival when rapamycin was applied to the radiated PSC27 cells. When exposed to mitoxantrone (MIT), a type

II DNA topoisomerase inhibitor frequently applied in clinics, prostate epithelial lines exhibited the uniform pattern as indicated by the *in vitro* survival assays (**Figure 7F**).

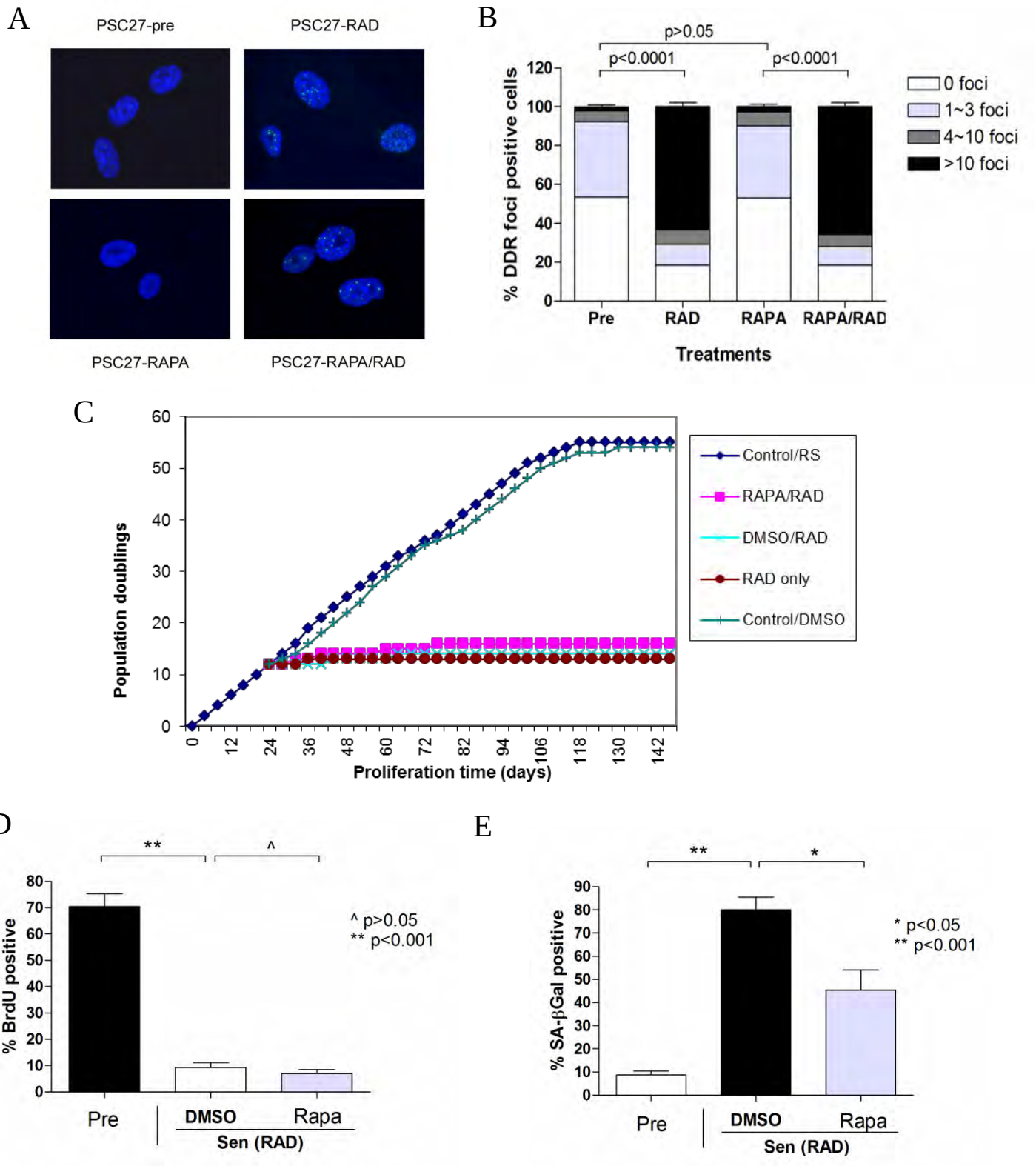

Figure 6. Rapamycin influences neither DNA damage lesions, senescence nor cell cycle arrest of human prostate fibroblasts. **A.** Immunofluorescence (IF) staining for a DNA damage marker-γH2AX, as the sensor of DNA double strand breaks. **B.** Senescence-associated damage foci (SADF) quantification of PSC27 cells after ionizing radiation. **C.** Proliferative potential of fibroblasts under several different conditions *in vitro*. **D.** Cell cycle progression arrested by DNA damage, measured by BrdU incorporation assay. **E.** Bright field staining of the senescence-associated βGal (SA-βgal), as a marker for cellular senescence and the relevant metabolic activities.

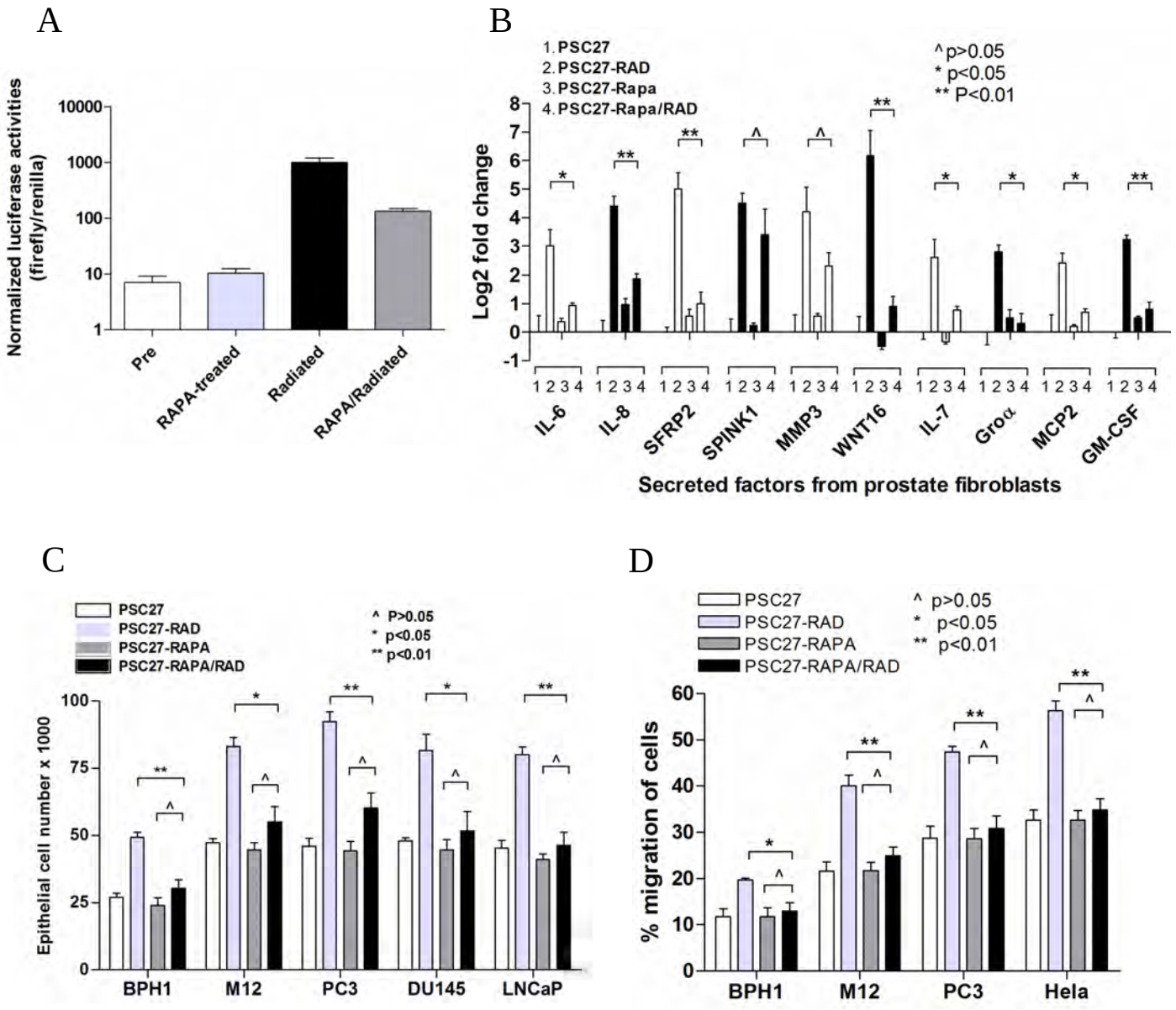

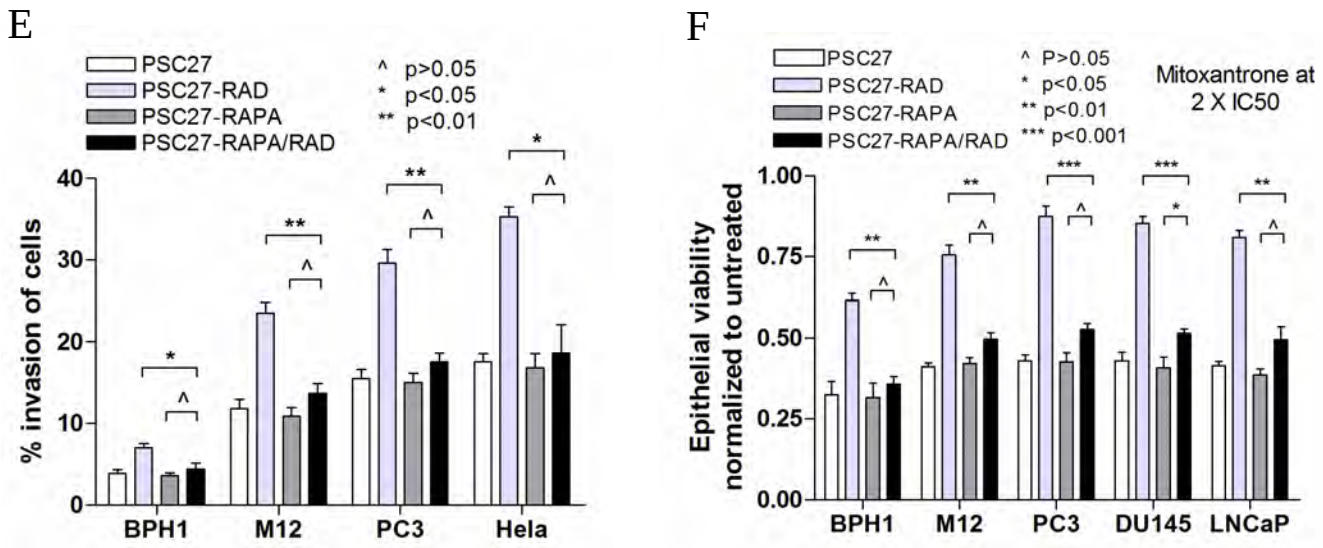

Figure 7. Rapamycin suppresses NF-κB activity, inhibits expression of multiple DDSP factors, and abrogates gain of proliferation, migration, invasiveness and chemoresistance of prostate cancer cells. **A** NF-κB activity assay by a reporter system. **B.** Gene expression profile of a group of typical DDSP factors at transcription level. Note, rapamycin was applied to a final concentration of 15 nM in culture after titration of a series of doses, a concentration established as an effective mTOR inhibitor but does not significantly inhibit cell proliferation and mitotic activities. **C.** Prostate cancer cell lines exhibited enhanced proliferation but in the case of rapamycin pre-treatment this tendency disappeared. **D.** Increased migration of prostate cancer cells was repressed by rapamycin pre-treatment. **E.** Promoted invasiveness was diminished upon rapamycin presence. **F.** Cells exhibited significant chemoresistance upon epithelial culture with CM from damaged prostate fibroblasts, which was deprived by the rapamycin pre-treatment of the latter.

Complex of mTOR/Raptor is a pivotal DDSP signaling node upon genotoxic stress and coordinates IKK/NF-κB pathway

The best characterized targets of mTOR phosphorylation are two protein families that control translation, namely ribosomal protein S6 kinases (S6K1 and S6K2 in mammals) and eukaryotic initiation factor 4E (eIF-4E) binding protein 1 (4EBP1). In mTORC1, raptor acts as a scaffolding protein, linking mTOR to S6K1 and 4EBP1 as a positive regulator of mTOR (Kopelovich et al., 2007). S6K1 is activated by phosphorylation and regulates ribosome biogenesis and protein translation, thus important in the control of cell proliferation and organism growth (Keniry and Parsons, 2011). In contrast, phosphorylation by mTOR inactivates 4EBP1. In quiescent cells, unphosphorylated 4EBP1 binds and inhibits eIF-4E as a rate-limiting key regulatory factor for protein synthesis. mTOR phosphorylation decreases the binding affinity of 4EBP1 for eIF-4E, which leads to increased translation of cap-dependent mRNAs (Yao et al., 2008).

Based on this, we looked at the status of mTOR pathway after IR. Typically, S6K1 was phosphorylated at T389, while 4EBP1 at S65, two well-known mTOR phosphorylation sites. In contrast, pre-treatment with rapamycin at an optimal concentration of 15 nM was able to diminish phosphorylation of S6K1 and reduce phosphorylated 4EBP1 (**Figure 8A**). This was in parallel to inhibition of mTOR activation, which is evidenced by phosphorylation at S2448

(Chiang and Abraham, 2005; Copp et al., 2009; Criollo et al., 2010) but suppressed by rapamycin in the culture conditions (**Figures 8A and 8B**). Upon DNA damage, phosphorylated mTOR was mainly localized the cytoplasm, with less signal in the nuclei. However, rapamycin dramatically suppressed phosphorylation of mTOR, as more apparent under damage conditions (**Figure 8B**).

Although expression of multiple secreted factors from damaged fibroblasts was significantly inhibited by rapamycin, the molecular mechanisms are unclear. To clarify this, we lysed cells 7~8 days after IR, and the lysates were immunoprecipitated with anti-mTOR, applied to SDS gel and blotted with mTOR, Raptor and IKK antibodies. Interestingly, DNA damage caused enhanced mTOR association with Raptor and IKKα, although the total amounts of these proteins in the lysates remain largely the same between before and after radiation (**Figure 8C**). While there was certain binding of mTOR to IKKβ and IKKγ, the signals remained generally weak and no major changes were observed (not shown). To confirm this, we applied reciprocal IP with IKKα antibody before collection of the pull-down products, and found increased mTOR but not Raptor association (**Figure 8C**). This indicates a distinct role for IKKα in the interaction with mTOR pathway, while aggregation of IKKα/β/γ and mTOR complex suggests the potential that NF-κB activation could occur through such an intermolecular interaction.

To determine the influence of rapamycin-caused mTOR suppression on NF-κB activities, we examined the cytoplasmic as well as nuclear expression of several factors. As is more compelling, the response of IKKα by phosphorylation at S176/180 is dramatically abrogated, even under DNA damage conditions (**Figure 9A**). This is in parallel with a large amount of IκBα reservation in the cytoplasm. Correspondingly, the downstream action-p65/p50 nuclear transportation largely vanished in the presence of rapamycin (**Figure 9A**).

With a reporter assay that measures NF-κB transcriptional activity, we found knockdown (KD) of either mTOR or Raptor can remarkably abolish the nuclear activity of such a transcriptional factor, although KD efficacy was even higher when siRNAs to mTOR and Raptor were applied synergistically. In comparison, a chemical treatment with rapamycin in the media generated similar results (**Figure 9B**).

Regulation of DDSP components by mTORC1 complex at translational level

Next, we asked whether mTOR effectors are crucial for DDSP factor synthesis/secretion. Although mTORC1 and C2 are both likely to be involved in regulation of the damage response, the former has been reported to be a major complex in cellular responses to multiple stimuli because its targets control Cap-dependent mRNA translation in mammalian cells (Choo et al., 2008). We used siRNA to deplete PSC27 cells of S6K1, or transfected the cells with a construct encoding exogenous 4EBP1, each case partially simulating the mTOR downstream target reaction upon mTOR inhibition by rapamycin. Interestingly, expression of most DDSP hallmarks including CXCL1, CCL8, WNT16B, IL-8, MMP12, SPINK1 and AREG) was dramatically attenuated or even abolished by such actions, and a similar consequence was observed when rapamycin was applied to cells (**Figure 9C**). Upon a cytokine based ELISA assay, extracellular yield of IL-8, a typical indicator of damage-induced secretion into the conditioned media of fibroblasts, was remarkably reduced when cells were subject to above treatments (**Figure 9D**). The combined action of S6K1 KD and 4EBP1 overexpression further augmented the reduction, and rapamycin caused a similar impact.

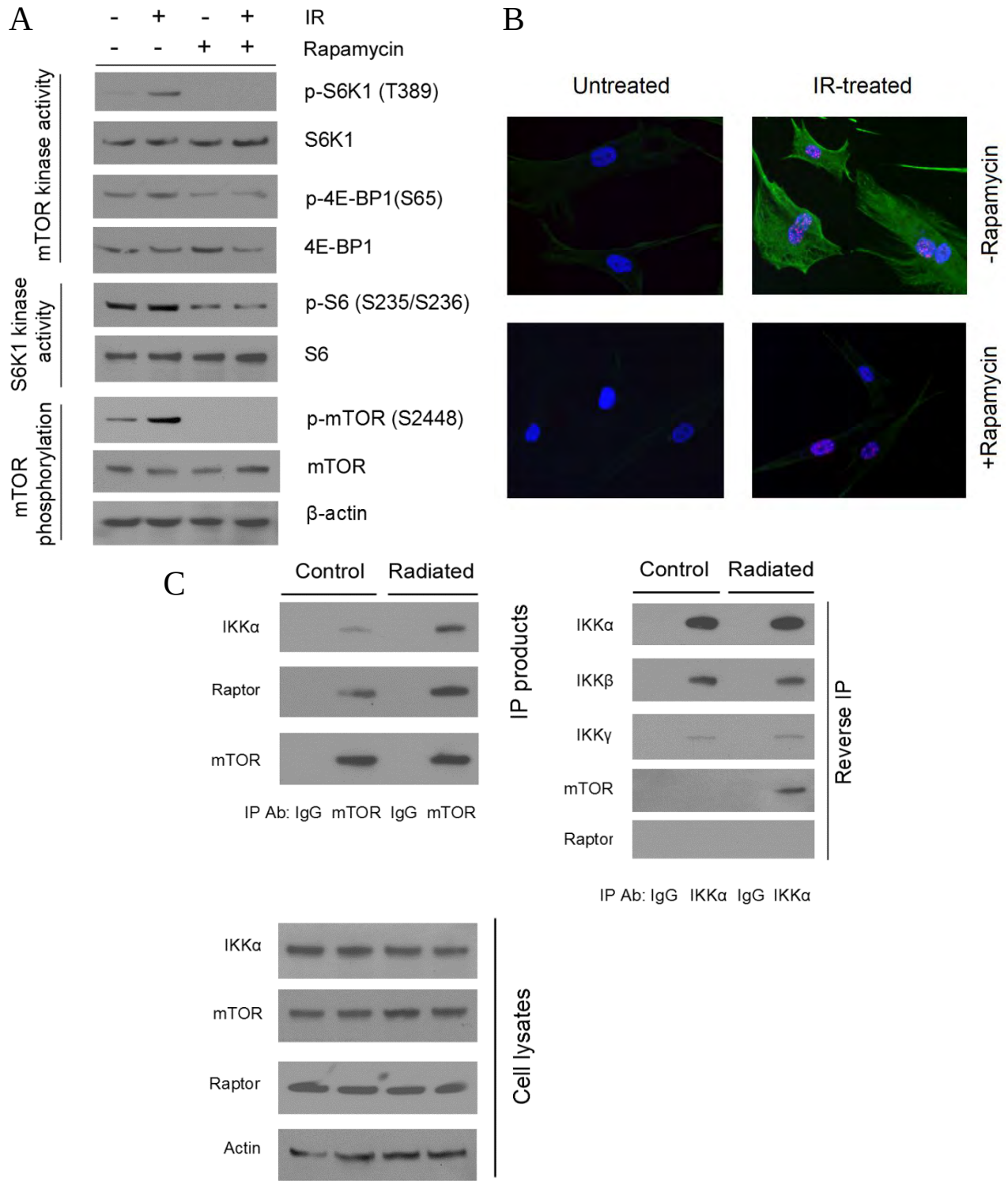

Figure 8. DNA damage engages the mTOR signaling pathway and subsequent interaction with IKK complex. **A.** Activated mTOR and its downstream targets in prostate fibroblasts upon ionizing radiation. **B.** Subcellular localization of DNA damage foci and subsequently phosphorylated mTOR in damaged cells. **C.** Molecular association of mTOR with the NF-κB regulator-IKK complex.

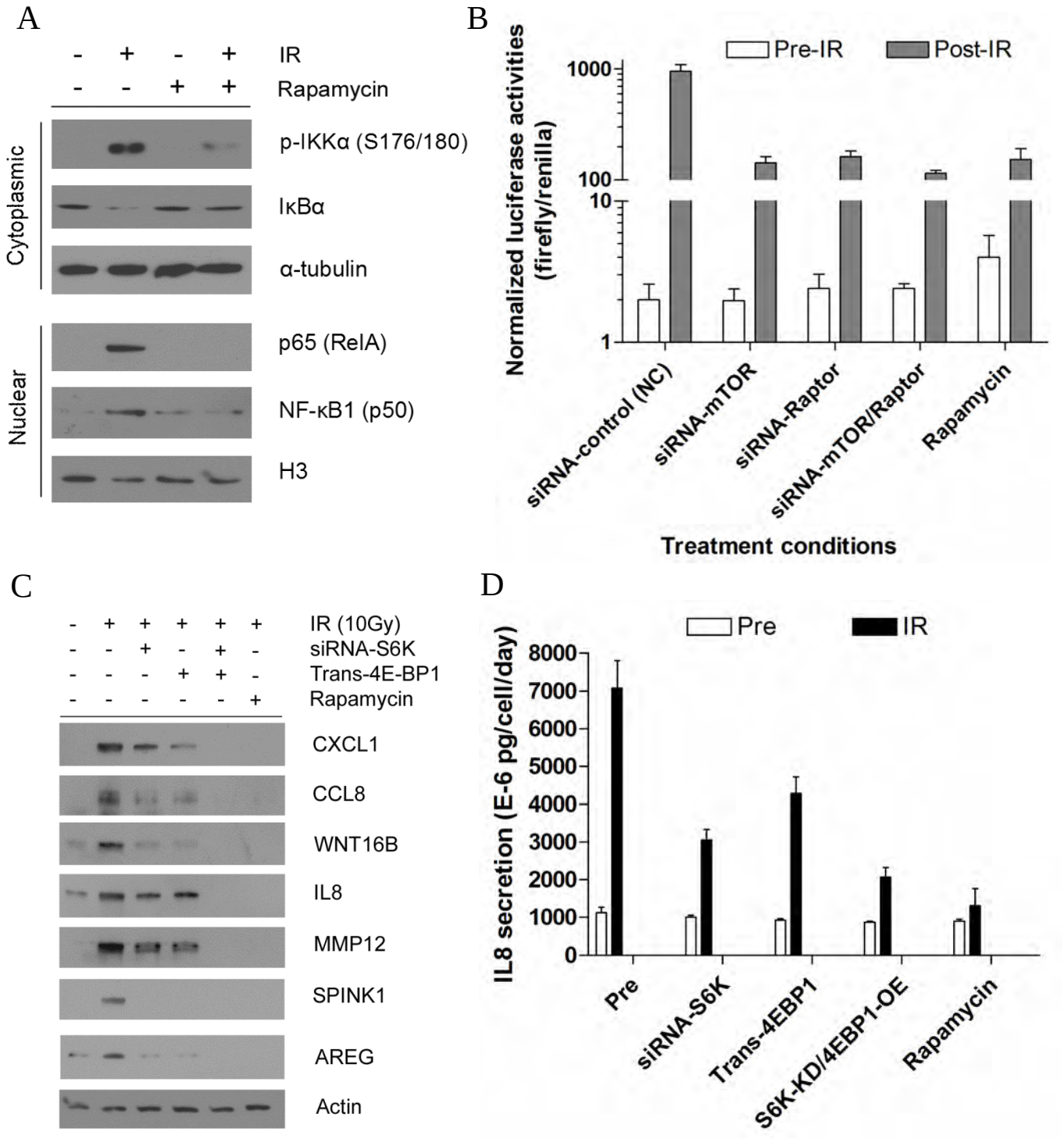

Figure 9. Rapamycin modulates NF-κB activity through discoupling the mTOR/Raptor complex formed in response to IR, and regulates DDSP factor translation via inhibiting direct targets of mTOR signaling (S6K1/4EBP1). **A.** Diminished NF-κB activation upon DNA damage stimulation at the presence of rapamycin. **B.** NF-κB activity reporter assay indicates that mTOR/Raptor modulates NF-κB activity in response to IR. Genetic deletion of mTOR and Raptor was applied in parallel to rapamycin treatment. **C.** Intracellular synthesis of several typical DDSP factors examined by immunoblots. **D.** Assessment of chemokine IL-8 production in conditioned media by ELISA assay.

Engagement of NF-κB signaling by the kinase activity of mTORC1 complex

To compare the potential implication of different IKK catalytic subunits in mediating mTOR signals upon IR treatment, we eliminated these two proteins individually with gene-specific small hairpin RNAs (shRNAs) before cells were subject to damage. Absence of α subunit substantially abrogated the nuclear activity of NF-κB, although the influence caused by β subunit KD was relatively higher. When both subunits were removed, IR could only induce minimal activation of NF-κB pathway (**Figure 10A**).

Thus, IKKα is likely to play an active role in relaying signals from activated mTORC1 complex. Does such an activation take place directly through an essentially straightforward intermolecular interaction or mediated by other factors involved in the damage response? To address this, we performed further examination. Briefly, PP242 is a novel, ATP competitive and selective inhibitor against mTOR kinase activity, with efficacy comparable to rapamycin in achieving cytoreduction, and apoptosis in multiple myeloma cells (Janes et al., 2010; Yang et al., 2013). To clarify whether mTOR directly phosphorylates IKKα, an *in vitro* assay was performed (Figure 5B). In this experiment, GST-mTOR and Flag-IKKα plasmids were co-transfected into PSC27 cells. Three hours prior to IR, cells were treated with PP242 to prevent phosphorylation of IKKα by experimentally activated mTOR. Seventy two hours after IR treatment, cells were lysed, and Flag-IKKα was IPed, with the IP products washed with the lysis better and with kinase buffer, successively. Products were then resuspended in kinase buffer and ATP was added to reaction mix. Since no exogenous mTOR was available following IP, all IKKα phosphorylation occurring during this assay must be due to co-precipitating mTOR protein.

After kinase reaction, the mix was immunoblotted with phosphorylated IKKα antibody. Under these conditions, IKKα was phosphorylated at position S176/180. To further confirm the kinase activity of mTOR on IKKα, we used calf intestinal phosphatase (CIP) for 45 min at 37 ℃ to treat the reaction mix, and eventually we did not see the phosphorylated IKKα antibody recognize CIP-treated IKKα (**Figure 10B**). Thus, the phosphorylation of IKKα is caused directly by activated mTOR under DDSP conditions, which is essentially reversible by dephosphorylation treatment. It is evident that physical association of mTOR with IKK complex takes place as one of the responses to environmental insults; IKKα is the major component that directly interacts with mTOR, while assemblying an overall IKK complex in damaged fibroblasts. Interestingly, when Rapamycin was used to replace PP242 in such series of treatment, lysis prior to kinase assay, neither co-precipitated mTOR nor the phosphorylated form (S176/180) of IKKα was observed (not shown), indicating a potential difference in the functional mode of these two mTOR inhibitors.

To further confirm that activated mTOR results in phosphorylation of such a catalytic IKK subunit as one of its targets, we analyzed the cell lysates by additional IP and immunoblots with phosphorylation-specific antibodies. The results indicated coexistence of two phosphorylated molecules isolated from the cell lysates at least since day 7 after cell damage (not shown). In addition, physical association of these proteins appeared to be present throughout 20 days post genotoxic treatment once such engagement is formed, although longer time binding is likely (not shown). Despite that fact that mTOR directly phosphorylates IKKα upon DDSP program activation, the functional relevance of IKKβ still remains elusive in a context of DNA damage to fibroblasts.

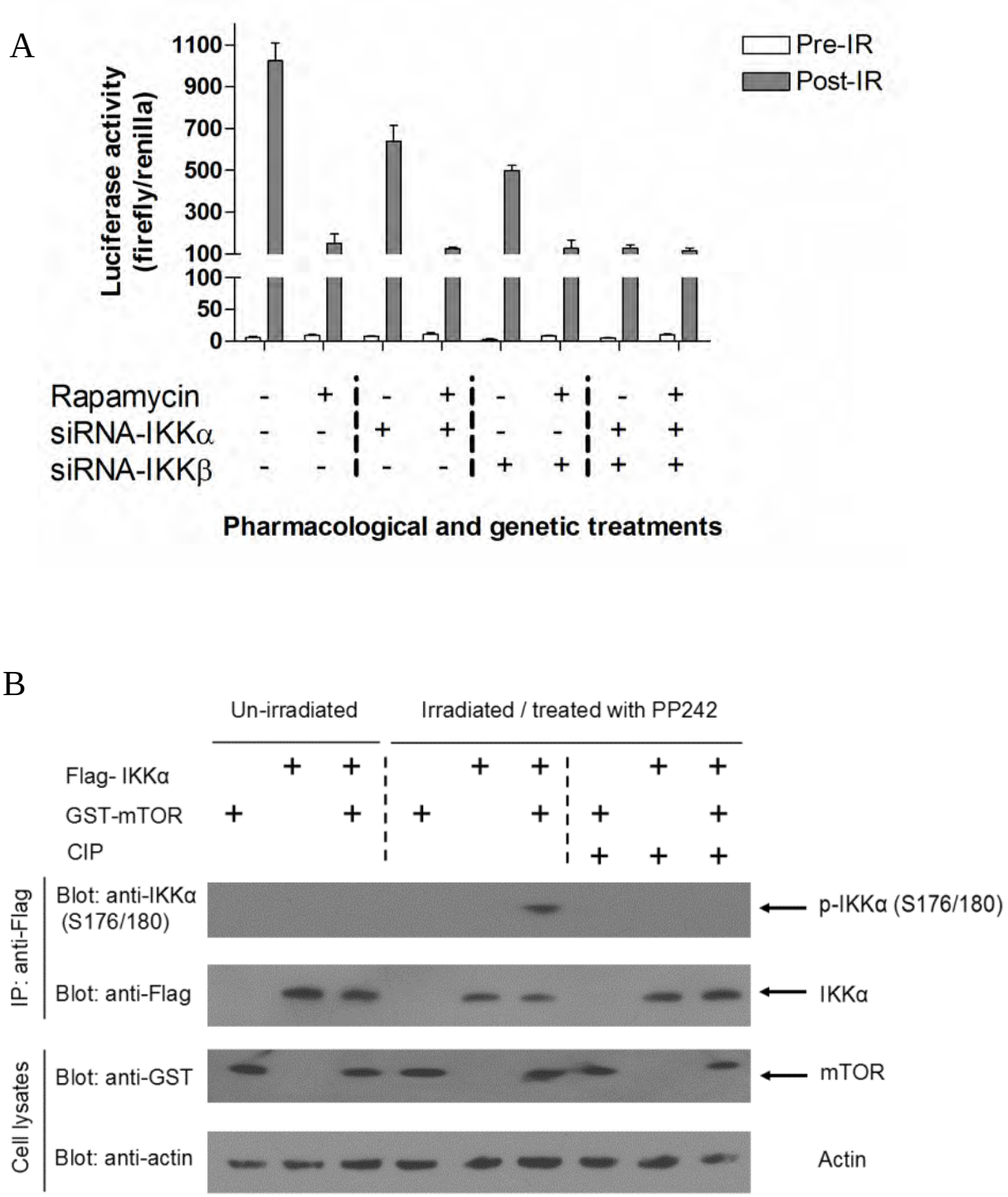

Figure 10. Physical and functional association of mTOR with IKK complex, as part of cellular responses to DNA damage events. **A.** Reporter assay of NF-kB upon genetic manipulation of IKK complex. **B.** Identification of IKKα as a substrate of mTOR-mediated phosphorylation through *in vitro* kinase assay.

Validation of differential involvement of IKK subunits in NF-κB signaling activation

It was reported that IL-1α is an important factor in the establishment and maintenance of secretion phenotype as part of fibroblast damage response (Orjalo et al, 2009). Cell surface-bound IL-1α is essential for signaling the senescence-associated secretion of IL-6 and IL-8, typical pro-inflammatory cytokines that reinforce growth arrest of senescence (Acosta et al., 2008). Senescent human fibroblasts express high levels of IL-1α mRNA, intracellular protein, and cell surface-associated protein, but secreted very little protein. Moreover, IL-1α can influence the DNA binding activity of NF-κB and C/EBPβ in senescent cells, thereby acting as a general and cell-autonomous regulator of senescence-associated secretion of a cytokine network. However, the functional connection between cell surface-bound IL-1α and damage-activated mTOR is largely unexplored.

To clarify this, we explored the influence of exogenous IL-1α on rapamycin-suppressed DDSP phenotype under damaging conditions. As an interesting point, IKKβ became phosphorylated in the fibroblasts after IR. Specifically, IL-1 receptor-associated kinase 1 (IRAK1) and IκBα are key components of the IL-1α/IL-1R signal pathway. After mediating IL-1R signaling, both of them are degraded (Orjalo et al, 2009). Assessment of this pathway status suggested that IRAK1 and IκBα decayed in damaged cells, but the protein levels were much higher upon rapamycin treatment, indicating a blockage of IL-1R signaling (**Figure 11A**). In contrast, addition of exogenous IL-1α to the media was able to reverse such a blockage, with the downstream molecular event-p65 and p50 nuclear translocation resumed to the original responsive state (**Figure 11A**).

In a relevant but opposite experiment, KD of IL-1α led to a reduced level of IKKβ phosphorylation, but phosphorylation of IKKα remains unchanged (**Figure 11B**). Although IRAK1 protein level was largely intact, IκBα amount decreased dramatically, implying active NF-κB signaling mediated by IKKα subunit. As a further support, nuclear signals of p65 and p50 were still clearly present, suggesting the continued activation of NF-κB complexes (**Figure 11B**).

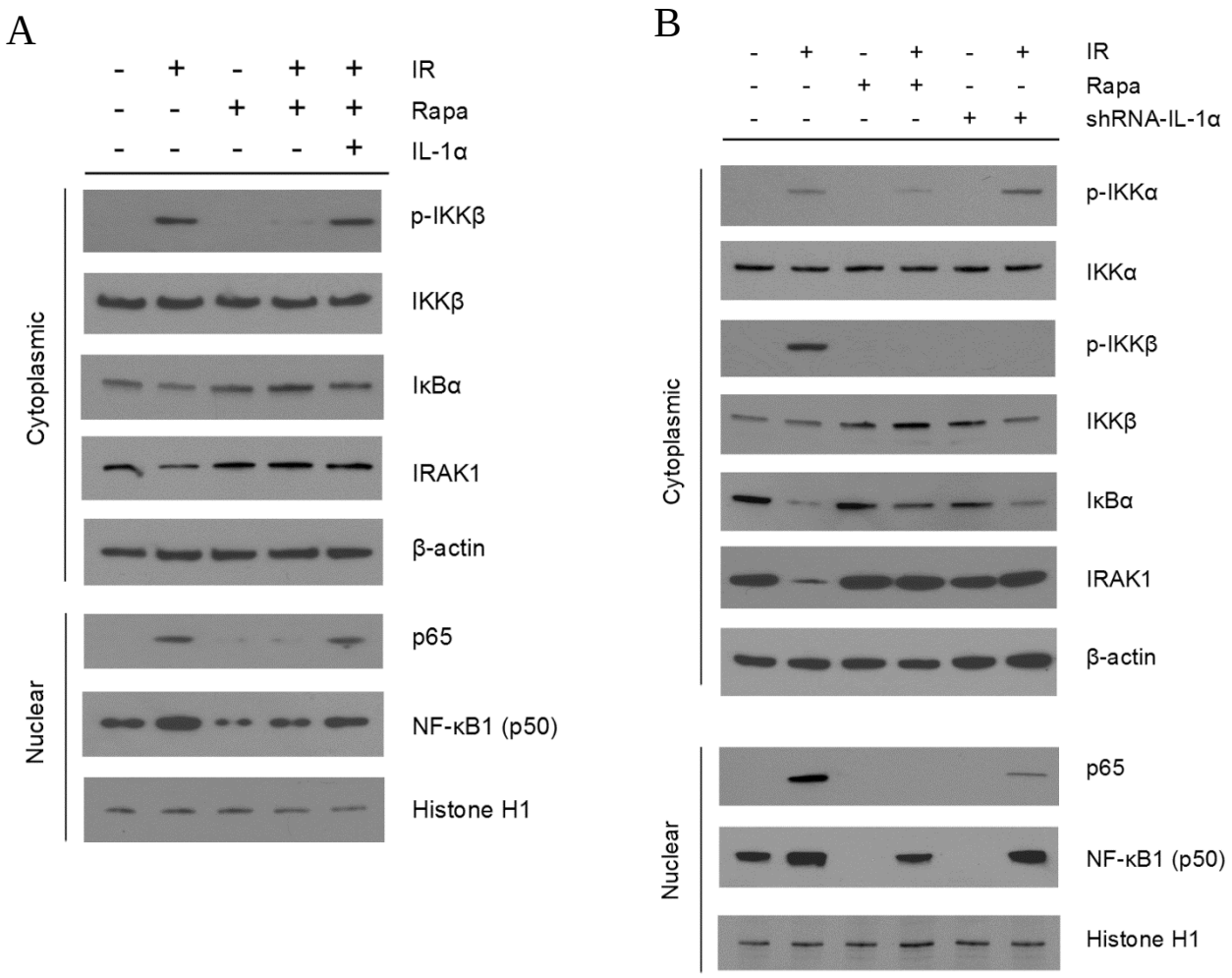

Figure 11. Differential involvement of IKK catalytic subunits in mediation of signal transduction upon genotoxic stress. **A.** Exogenous IL-1α rescues rapamycin-suppressed DDSP phenotype under damaging conditions. **B.** Elimination of IL-1α from stromal cells does not abrogate DDSP phenotype generated by DNA-damaging agents.

Functional roles of Akt and PI3K in mediating DNA damage signal transduction to mTORC1

Next, we asked whether the upstream regulator of mTOR in mammalian cells-Akt, is pivotal for such DDSP-associated mTOR activation. Application of MK-2206, a highly selective non-ATP competitive allosteric pan-Akt inhibitor (against Akt1, Akt2 and Akt3) thus of a broad preclinical antitumor activity (Kim et al., 2011), not only abolished IR-induced Akt phosphorylation, but increased the radiosensitivity of glioblastoma multiforme U87MG cells (Li et al., 2009). In our studies, chemical treatment with MK-2206 to PSC27 cells leads to diminished mTOR phosphorylation, which is in parallel with reduced Akt phosphorylation at S473 (**Figure 12A**). However, p38 MAPK status change remained largely the same no matter if Akt is down or not; that is, once fibroblasts are exposed to DNA damage, this MAPK stay consistently activated.
In a similar experiment, the phosphatidylinositol 3-kinase-PI3K was found to be of similar role in mediating the signals from damaged DNA. Knockdown of the catalytic subunit p110 was able to diminish Akt phosphorylation, mTOR phosphorylation, although the PI3K regulatory subunit p85α remain largely unchanged (**Figure 12B**). Again, in such a treatment p38 phosphorylation, an indicator of MAPK pathway activation remained constantly active.

As the downstream hallmark of a DDSP event, nuclear translocation-mediated activity of NF-kB was remarkably dampened by either PI3K elimination or Akt inhibition, although there was still some nuclear activity remaining upon exposure of fibroblasts to IR (**Figure 12C**). It is thus likely that either signaling from other upstream regulators alternative to p38-mediated pathway is simultaneously present, or p38 mediates its own signaling exclusively from PI3K/Akt pathway but eventually engage NF-kB complex in damaged cells.

***In vivo* manipulation of DDSP sensitizes tumors to chemotherapy through restraining cancer cell repopulation**

In addition to the above *in vitro* studies, examination of mTOR regulation of DDSP through manipulation of fibroblasts before tissue recombination was performed. Upon IR treatment, PSC27 cells were incubated with rapamycin for 8 days before they were combined with PC3-Luc (a PC3-derived subline that overexpresses firefly luciferase) cells and transplanted to subcutaneous areas. At the endpoint of an 8-week period, mice were handled for bioluminescence imaging with IVIS xenogeny system, with tumor size measured for further analysis (not shown). Statistically, PC3 tumor growth was inhibited by ~50%, through such a pre-treatment with rapamycin under *in vitro* conditions to PSC27-RAD cells (not shown). Note, in such a treatment protocol, there was no MIT or other DNA-damaging agents administered. Thus, a single and early dose of this compound was potent to prevent a full development of DDSP-conferred tumor growth.

In another treatment group, preclinical studies mimicking physiological reality were performed. Starting from the 3rd week, mice received mitoxantrone at a dose of 0.2 mg/kg by intraperitoneal injection on day 1 of week 3, week 5, and week 7. Thus, a total regimen of 3 × 2-week cycles was administered. After the final treatment cycle the mice were handled for bioluminescence imaging (not shown). In such a course, rapamycin was given at 0.1 mg/kg every other day since the beginning of MIT injection, after a dosing phase performed in advance to minimize its direct effect on the growth of tumors composed of PC3 cancer cells exclusively per se. Our *in vitro* studies demonstrated that rapamycin inhibits the impact of DDSP to stimulate cancer cell

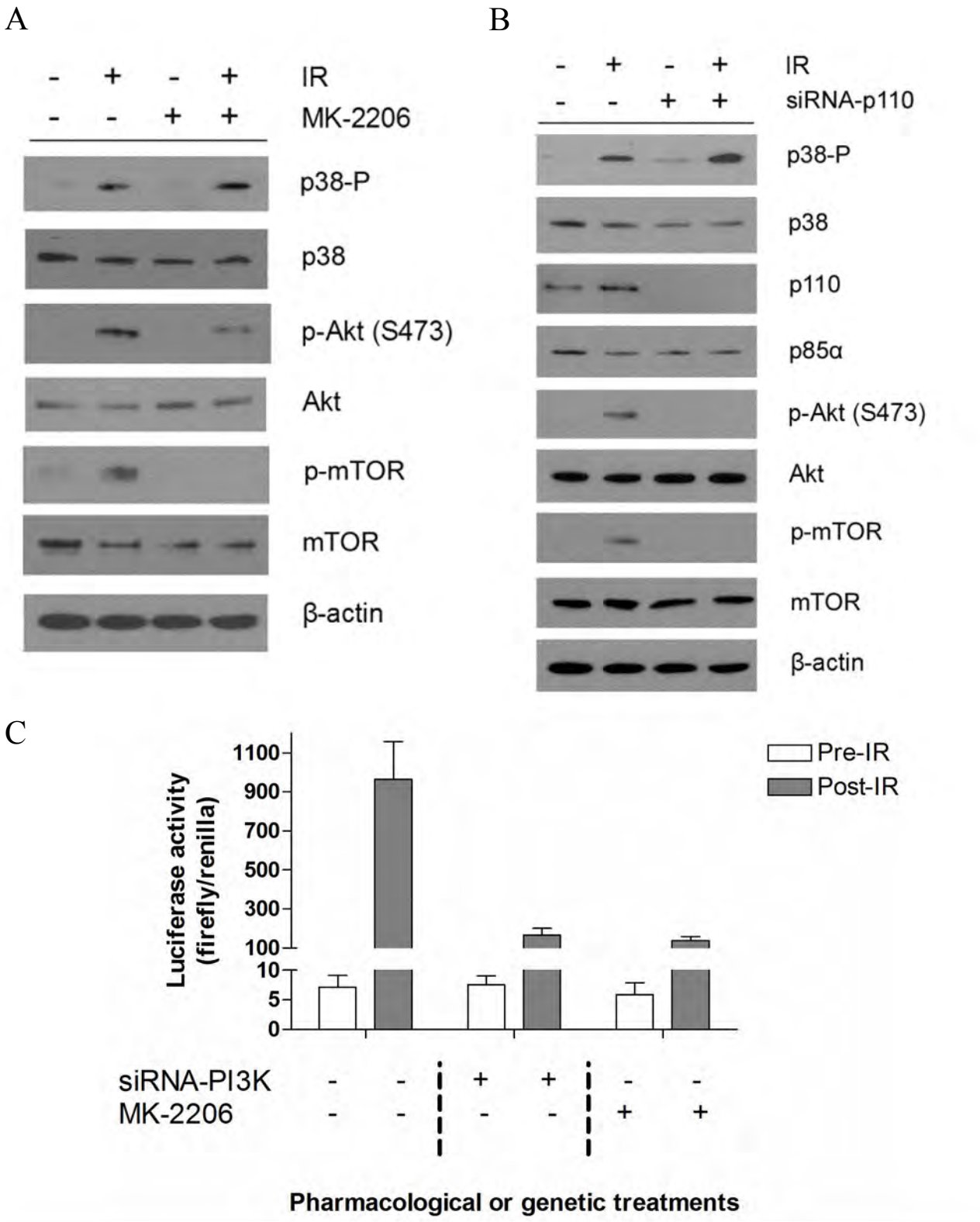

Figure 12. Akt and PI3K are implicated in relaying damage signals to the downstream NF-kB complex. **A.** Chemical inhibition of Akt leads to diminished mTOR activation. **B.** Genetic elimination of PI3K reduces Akt/mTOR signaling in damaged fibroblasts under a DDSP context. **C.** Reporter assay of NF-kB activity indicates that PI3K and Akt are essential to modulate NF-κB signaling in response to IR.

A

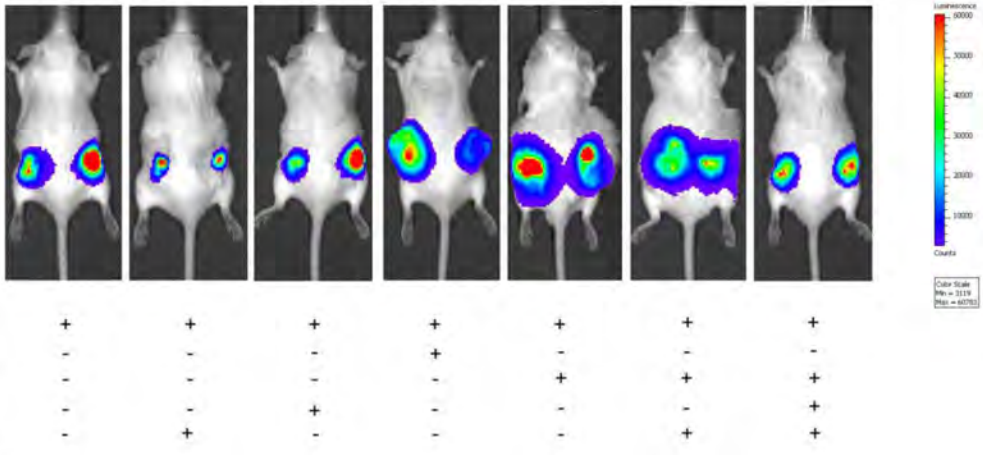
PC3 + + + + + + +
PSC27 - - - + - - -
PSC27-RAD - - - - + + +
Rapa - - + - - - +
Chemo (MIT) - + - - - + +

B

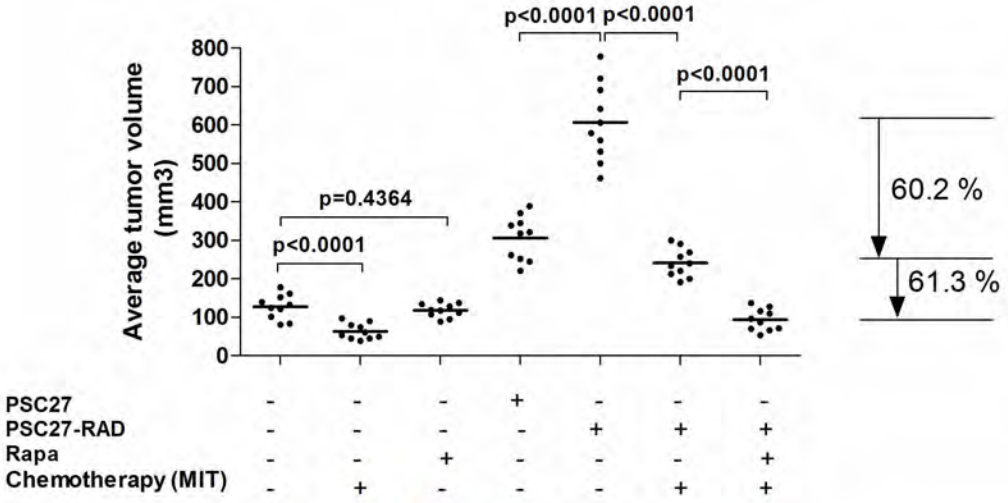
Average tumor volume (mm3)
800
700
600
500
400
300
200
100
0
p<0.0001 p<0.0001
p<0.0001
p=0.4364
p<0.0001
60.2 %
61.3 %
PSC27 - - - + - - -
PSC27-RAD - - - - + + +
Rapa - - + - - - +
Chemotherapy (MIT) - + - - - + +

C

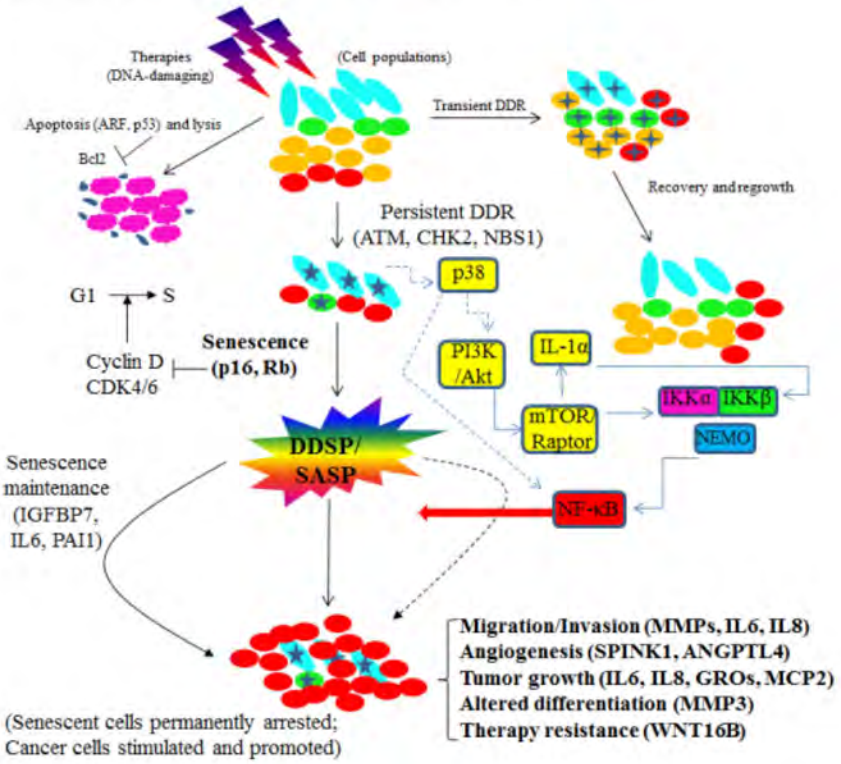
Therapies (DNA-damaging)
(Cell populations)
Transient DDR
Apoptosis (ARF, p53) and lysis
Bcl2
Recovery and regrowth
Persistent DDR (ATM, CHK2, NBS1)
p38
G1 → S
Cyclin D CDK4/6
Senescence (p16, Rb)
PI3K /Akt
IL-1α
IKKα IKKβ
mTOR Raptor
NEMO
DDSP/ SASP
NF-κB
Senescence maintenance (IGFBP7, IL6, PAI1)
Migration/Invasion (MMPs, IL6, IL8)
Angiogenesis (SPINK1, ANGPTL4)
Tumor growth (IL6, IL8, GROs, MCP2)
Altered differentiation (MMP3)
Therapy resistance (WNT16B)
(Senescent cells permanently arrested; Cancer cells stimulated and promoted)

Figure 13. Preclinical evidence that treatment-induced resistance is diminished by rapamycin administration. **A.** PC3 tumor growth upon transplantation to SCID mice in an 8-week period. Representative bioluminescence images are shown. **B.** Quantitative measurement of tumor growth with or without combinational treatment of mitoxantrone and rapamycin, as administered in (A) conditions. **C.** Schematic depicting tumor-stromal interactions in TME upon therapeutic DNA damage. Upon minor damage by chemotherapy or radiation (e.g. 0.5 Gy) DDR foci disappear from cells within hours after complete repair. In contrast, at higher doses (≥5 Gy), most damage foci in stromal cells persist for longer period, and cells develop typical senescence. Concurrently, majority of cancer cells are sensitized to such major damage and enter the rapid death programs including apoptosis and/or autophagy. High dosage of DNA damage usually triggers a persistent DDR engaging ATM, CHK2 and NBS1 which activate the cell cycle effectors p53/p16/RB, and leads to continuous and robust secretion of a large spectrum of proteins, a phenomenon coined as the DNA damage secretory phenotype (DDSP). A few secreted factors function in a cell-autonomous manner, such as IGFBP7, IL6, PAI1, which can maintain and reinforce the senescent state through a positive feedback loop that sustains the DDR. Several inflammatory cytokines (CSF1, MCP1, CXCL1), act in a cell non-autonomous manner, potentiate regression of a tumor by activating the innate immune response that promotes tumor clearance. However, most components of the secretory phenotype are actively involved in cancer-promotion by cell non-autonomous mechanisms, involving enhanced migration, invasiveness, angiogenesis, accelerated cancer growth, altered epithelial differentiation (MMP-3), and epithelial-mesenchymal transition (EMT, including IL6, IL8 and recently reported WNT16B which specifically engages a EMT cascade in epithelial cancer cells). All of these contribute to a more malignant phenotype, namely acquired therapy resistance within TME. Once transformed by such a program, cancer cells are therapeutically more refractory. As an important signal network node, mTOR activates downstream pathways both transcriptionally and post-translationally, generating a sustained framework of DDSP secretion in the tumor-adjacent but

proliferation, it is thus critical to proceed to qualify mTOR as a potential therapeutic target for *in vivo* DDSP modulation. At the endpoint of an 8-week period, rapamycin-treated group formed significantly smaller tumors than the placebo-treated mice (**Figure 13A**). To validate the preclinical efficacy, we analyzed the data statistically and found beyond the 60.2% of tumor shrinkage by MIT itself, rapamycin administration resulted in an additional 61.3% reduction of tumor burden (**Figure 13B**), which is essentially in line with the effect of this agent in diminishing DDSP-generated chemoresistance of PCa cell lines *in vitro*.

In the time course of thoroughly delineating functional roles of mTOR/NF-κB axis in mediating DDSP signaling cascade, comprehensive studies of several other molecules including γH2AX (genetic depletion), ATM (KU55933), p38 (SB203580; LY2228820) and HSP27 (genetic eliminationon) are intensively carried out in our lab, with relevant data to be reported systematically in future.

KEY RESEARCH ACCOMPLISHMENTS

- An anti-WNT16B mouse monoclonal antibody was purified through optimized column chromatography technique and renaturing procedures. The *in vitro* experiments demonstrated that the antibody is biologically active and has even higher capacity in recognizing WNT16B as an antigen expressed from human fibroblasts.
- Upon application to cell culture conditions, anti-WNT16B significantly reduced the proliferative gain of prostate cancer epithelial cells conferred by WNT16B overexpressed from a stable human fibroblast line; dramatically neutralized the growth augment exerted by the full DDSP of damaged prostate fibroblasts; and prominently abolished the invasiveness of cancer cells upon treatment with conditional media of fibroblasts upon DNA damaging.
- Pilot xenograft models comprising PCa (PC3/VCaP) implanted with PSC27 were established, and examination of tumor responses to single agent or combination therapy indicated the efficacy of synergistic treatment in minimizing tumor malignancy.
- A group of primary fibroblast cell lines was isolated and established from the prostate tissue of mice with FVB background. Expression of the typical cell lineage-specific markers confirmed their stromal origin, and typical DDSP phenotype is developed upon DNA damaging treatment. However, as is reminiscent of our previous data from human fibroblasts, the upregulation of a handful DDSP effectors persisted even overexpression of majority of soluble factors is suppressed by pathway-targeting chemicals, implying the highly complex nature of this program and complication of a large molecular network that is engaged in the initiation and maintenance of this stroma-specific response under genotoxic conditions.
- The unique spectrum and extent of DDSP generated upon DNA damage as compared to alternative mechanisms that employ non-genotoxic scenario was characterized in our preliminary work, and continued studies are expected to reveal the critical or master signal node(s) that allow demarcation of these distinct phenotypes .
- Optimal cells and treatments to initiate damage response were determined.
- Pathways of potentially critical mediators of DDSP response were modulated, with mTOR/NF-κB studied as an exemplary pilot.
- The influence of key regulators, including but not limited to mTOR/NF-κB complexes in mediating adverse carcinoma phenotypes through paracrine effects of the TME was demonstrated.
- The *in vivo* efficacy of other DDSP master regulators are to be determined through the model system we've established to date, and will allow to gain insightful understanding of mechanisms underlying such a cell non-autonomous response to anti-cancer therapeutic approaches.

REPORTABLE OUTCOMES

- Zhang, B. and **Sun, Y.** Landscape and Targeting of the Angpt-Tie System in Current Anticancer Therapy. ***Translational Medicine.*** 2015. Accepted.
- **Sun, Y.** Tumor Microenvironment and Cancer Therapy Resistance. ***Cancer Lett.*** 2015. (Special issue) Accepted.

- Laberge, R. M., **Sun, Y.,** Orjalo, A. V., Patil, C. K., Freund, A., Zhou, L., Curran, S. C., Davalos, A. R., Wilson-Edell, K. A., Liu, S., Limbad, C., Demaria, M., Li, P., Hubbard, G. B., Ikeno, Y., Javors, M., Desprez, P. Y., Benz, C. C., Kapahi, P., Nelson, P. S. and Campisi, J. 2015. mTOR regulates the pro-tumorigenic senescence-associated secretory phenotype by promoting IL1A translation. ***Nat. Cell. Biol.*** 2015. 17: 1049-1061.
- Chen, F., Zhuang, X., Lin, L., Yu, P., Wang, Y., Shi, Y., Hu G. and **Sun, Y.** New Horizons in the Tumor Microenvironment Biology: Challenges and Opportunities. ***BMC Medicine.*** 2015. 13: 45. (highly accessed and journal-featured article)
- **Sun, Y.** 2015. Translational Horizons in the Tumor Microenvironment: Harnessing Breakthroughs and Targeting Cures. ***Med. Res. Rev.*** 35: 408-436. (cover page article)
- Chen, F., Qi, X., Qian, M., Dai, Y. and **Sun, Y.** 2014. Tackling the Tumor Microenvironment: What Challenge Does It Pose to Anticancer Therapies? ***Protein Cell.*** 5: 816–826.
- **Sun, Y.**, Coleman, I., and Nelson. P. The Mammalian Target of Rapamycin is an Essential Node of Signaling Network that Steers the Tumor Microenvironment-Derived DNA Damage Secretory Program. (Identification of mTOR as a novel target for therapeutic intervention to abrogate resistance mechanisms derived from the tumor microenvironment, in preparation)
- **Sun, Y.** 2015. Tackling the damaged tumor microenvironment: what challenge does it pose to anticancer therapies? 8th annual World Cancer Congress (WCC). Theme: Bridging Research and Practice. Beijing, China (**Co-Chair of Session 404: Cancer/Tumor Microenvironment Interactions; invited talk**)
- **Sun, Y.**, Coleman, I., Plymate, S. and Nelson, P. 2014. DNA damage response in quiescent fibroblasts elicits a distinct secretory program and confers acquired resistance to cancer therapies. San Diego, CA. 105th AACR Annual Meeting. Abstract, Poster.

CONCLUSIONS

The development of resistance to chemotherapy and radiation is a major obstacle for lasting effective treatment of cancers. Significant progress has been made to elucidate the mechanisms of DDSP response, and exploration of the likelihood to improve therapeutic efficacy by targeting this phenotype is promising. However, selection of the appropriate target to substantially prevent or minimize DDSP-conferred treatment resistance stays on the top of most challenging and clinically relevant questions. Characterization of mTOR-mediated DDSP development upon DNA damaging conditions sheds light on the regulatory mechanisms of this cell non-autonomous program by showing that mTOR is a functionally pivotal node and relays signals from DNA strand breaks to ensuing events in TME that are exposed to therapeutic insults, either physically or chemically.

Therapy-induced secretory phenotype is featured by the resistance acquired from DNA-damaged host stromal cells to neoplastic cells for survival in treatment situations

DNA damaging regimens involve the systemic administration of genotoxic compounds or radiation that induces cancer cell death via well-established DNA damage response signaling networks. Less understood is how the treatment of other cell types within the tumor microenvironment affects the therapeutic response. Here we discuss the recent work by showing that tumor-adjacent stromal cells can respond to genotoxic stress by activating a paracrine secretory program, which is mediated by a signaling cascade. Although this secretory response serves to protect progenitor cells and promote tissue regeneration in conditions of cellular stress,

it can also be utilized by tumor cells to survive frontline chemotherapy (Gilbert and Hemann 2011). Thus, local pro-survival signaling may present a fundamental barrier to tumor clearance by genotoxic agents, suggesting that effective treatments need to target both cancer cells and the tumor microenvironment.

In many cases, drug-induced antitumor activity occurs rapidly following therapeutic administration. A secretory response occurs acutely, which is particularly universal for hematopoietic malignancies, where tumor clearance frequently occurs within 1 to 2 days of treatment. For instance, release of IL-6 from both human and mouse endothelial cells in the thymus is within 24 hours of treatment, suggesting some secretory response is engaged rapidly enough to influence tumor response to DNA damage, as acute stress–associated phenotype (ASAP) (Gilbert and Hemann 2011). However, distinct from such ASAP, a robust and long term secretory phenotype in solid tumors that are more indirectly engaged in response to therapies is the DNA damage-associated secretory phenotype (DDSP) (to be filled). The DDSP develops gradually over the course of 7 to 15 days and reaches climax usually after prominent markers of senescence are detected. Although ASAP can influence therapeutic efficacy acutely, its relevance is usually limited and applicable to predominant clinical settings such as metronomic chemotherapy, where therapy is applied in an ongoing manner over a period of cycles (Pasquier et al., 2010). In contrast, DDSP represents a TME-specific stress response in which stromal cells sense DNA damage and gradually activate a cytoprotective secretory program, protecting both normal and cancer cells in the pathological tissue milieu from cell death. Under such conditions, cancer cells can take advantage of comprehensive and general stress-induced secretory responses that presumably have evolved to promote normal tissue repair and regeneration, to survive and progress after administration of frontline chemotherapy in a chronical manner.

Selective targeting mTOR using rapamycin to control DDSP effector expression at post-translational level illustrates novel therapeutic avenues

The mTOR serine/threonine kinase is present in two cellular protein complexes, TORC1 and TORC2, which have distinct subunit composition, substrates and mechanisms of activation (Abraham, 2009; Guertin, and Sabatini, 2007). The best-known substrates of TORC1 are S6 kinase (S6K) and 4EBP1 (eukaryotic initiation factor 4E-binding protein-1); the main substrates of TORC2 are AKT and related kinases. Rapamycin (sirolimus) and its analogs, such as RAD001 (everolimus) and CCI-779 (temsirolimus), suppress mTOR activity through an allosteric mechanism that acts at a distance from the ATP-catalytic binding site (Guertin and Sabatini, 2009). Members of this class of mTOR inhibitor have profound immunomodulatory activity and have achieved considerable success as anticancer agents (Janes and Fruman, 2009; Thomson et al., 2009). Mechanistically, rapamycin suppresses TORC1-mediated p70S6K activation, but does not acutely inhibit TORC2; it also reduces phosphorylation of 4EBP1, although only partially in many cell contexts (Janes et al., 2010). mTORC1 is composed of mTOR, Raptor, mLST8, PRAS40, and Deptor. Nutrient availability regulates mTORC1 in its ability to phosphorylate p70S6K and 4EBP1 in order to induce protein synthesis (Zoncu et al., 2011). In addition to regulating protein synthesis, the mTORC1 complex attenuates insulin signaling by negatively regulating IRS1 and activating GRB10 (Shah and Hunter, 2006; Yu et al., 2011; Hsu et al., 2011). The mTORC2 complex, in contrast, contains mTOR, Rictor, mLST8, Deptor, SIN1, and Protor, and its targets include AKT, PKCα, and SGK1, which regulate cellular

growth and survival (Zoncu et al., 2011). The central role of mTOR in these growth regulatory events makes it a rational target for cancer therapy.

Our data indicate that genetic elimination of Raptor is potent enough to diminish majority of overexpressed DDSP effectors, mainly through dephosphorylation of both p70S6K and 4EBP1, two major targets of mTORC1. Pharmacologically, even when rapamycin is applied at a concentration of 15 nM in the culture, phosphorylation of these mTORC targets was significantly reduced, suggesting the relatively high sensitivity of stromal cells. In addition, the chemoresistance of PCa cell lines acquired from damaged stromal cells was markedly decreased, once the latter was subject to rapamycin treatment. So far, activation of mTOR has been found to be associated with resistance to chemotherapy and radiotherapy (Jiang and Liu 2008). However, implication of mTOR in mediating DNA damage signals to its downstream molecules has not been thoroughly explored, especially in the background of stromal-epithelial interactions. Thus, our study provides a novel perspective in determination of the biological role of mTOR in depriving resistance of cancer cells conferred by damaged host stromal cells under therapeutic conditions.

The combination of mTOR inhibitors with other DNA-targeting agents is likely a promising approach, which may have synergistic effects in tumor growth inhibition thus allowing control of the potential of cancer cell repopulation conferred from certain pathological niches after treatment. The preclinical data from our experimental animal models indeed suggests that rapamycin administration can effectively modulate prostate cancer resistance in the course of a chemotherapy regimen composed of multiple waves of dosing. Pharmacological control of mTOR activation upon DNA-damaging therapies is therefore a strong inspiration to promote cancer patient treatment outcome by depriving therapy-conferred resistance.

REFERENCES

Abraham, R. T. 2009. Regulation of the mTOR signaling pathway: from laboratory bench to bedside and back again. F1000 Biology Reports 1: 8.

Acosta, J. C., O'Loghlen, A., Banito, A., Guijarro, M. V., Augert, A., Raguz, S., Fumagalli, M., Costa, M. D., Brown, C., Popov, N., et al. 2008. Chemokine signaling via the CXCR2 receptor reinforces senescence. Cell. 133: 1006-1018.

Bartek, J., Hodny, Z. and Lukas, J. 2008. Cytokine loops driving senescence. Nat. Cell Biol. 10: 887-889.

Bel-Ochi, N. C., Bouratbine, A., Mousli, M., 2013. Enzyme-Linked Immunosorbent Assay using Recombinant SAG1 Antigen to Detect Toxoplasma gondii-Specific Immunoglobulin G Antibodies in Human Sera and Saliva. Clin Vaccine Immunol. 20: 468-473.

Ben-Neriah, Y. and Karin, M. 2011. Nat. Immunol. 12: 715–723.

Bleau, A. M., Hambardzumyan, D., Ozawa, T., Fomchenko, E. I., Huse, J. T., Brennan, C. W., and Holland, E. C. 2009. PTEN/PI3K/Akt pathway regulates the side population phenotype and ABCG2 activity in glioma tumor stem-like cells. Cell Stem Cell. 4: 226–235.

Bonizzi, G. and Karin, M. 2004. The two NF-κB activation pathways and their roles in innate and adaptive immunity. Trends Immunol. 25:280–288.

Burgess, R. R. 2009. Refolding solubilized inclusion body proteins. Methods Enzymol.17: 259–282.

Cabrita, L. D. and Bottomley, S. P. 2004. Protein expression and refolding—a practical guide to getting the most out of inclusion bodies. Biotechnol. Annu. Rev.10: 31–54.

Campisi, J., Andersen, J. K., Kapahi, P, and Melov, S. 2011. Cellular senescence: A link between cancer and age-related degenerative disease? Seminars in Cancer Biology. 21: 354-359.

Chiang, G. G. and Abraham, R. T. 2005. Phosphorylation of Mammalian Target of Rapamycin (mTOR) at Ser-2448 Is Mediated by p70S6 Kinase J. Biol. Chem. 280: 25485-25490.

Chien, Y., Scuoppo, C., Wang, X., Fang, X., Balgley, B., Bolden, J. E., Premsrirut, P., Luo, W., Chicas, A., Lee, C. S., Kogan, S. C. and Lowe, S. W. 2011. Control of the senescence-associated secretory phenotype by NF-κB promotes senescence and enhances chemosensitivity. Genes Dev. 25: 2125–2136.

Choo, A. Y., Yoon, S. O., Kim, S. G., Roux, P. P. and Blenis, J. 2008. Rapamycin differentially inhibits S6Ks and 4E-BP1 to mediate cell-type-specific repression of mRNA translation. PNAS. 105: 17414-17419.

Copp, J., Manning, G. and Hunter, T. 2009. TORC-Specific Phosphorylation of Mammalian Target of Rapamycin (mTOR): Phospho-Ser^{2481} Is a Marker for Intact mTOR Signaling Complex 2. Cancer Res. 69: 1821-1827.

Criollo, A., Senovilla, L., Authier, H., Maiuri, M. C., Morselli, E. et al. 2010. The IKK complex contributes to the induction of autophagy. EMBO J. 29: 619-631.

Dan, H. C., Adli, M., and Baldwin, A.S. 2007. Regulation of mammalian target of rapamycin activity in PTEN-inactive prostate cancers by IKKα. Cancer Res. 67: 6263–6269.

Dan, H. C. and Baldwin, A. S. 2008. Differential Involvement of IκB Kinases α and β in Cytokine- and Insulin-Induced Mammalian Target of Rapamycin Activation Determined by Akt. J Immunol. 180: 7582-7589.

Dan, H. C., Cooper, M. J., Cogswell, P. C., Duncan, J. A., Ting, J. P. Y. and Baldwin, A. S. 2008. Akt-dependent regulation of NF-κB is controlled by mTOR and Raptor in association with IKK. Genes Dev. 22: 1490-1500.

Demidenko Z. N., Zubova, S. G., Bukreeva, E. I., Pospelov, V. A., Pospelova, T. V. and Blagosklonny, M. V. 2009. Rapamycin decelerates cellular senescence. Cell Cycle. 8: 1888-1895.

Engelman, J. A., Luo, J. and Cantley, L. C. 2006. The evolution of phosphatidylinositol 3-kinases as regulators of growth and metabolism. Nat. Rev. Genet. 7: 606–619.

Ferbeyre, G., de Stanchina, E., Querido, E., Baptiste, N., Prives, C. and Lowe, S. W. 2000. PML is induced by oncogenic ras and promotes premature senescence. Genes Dev. 14: 2015–2027.

Foster, K. G., and D. C. Fingar. 2010. Mammalian target of rapamycin (mTOR): conducting the cellular signaling symphony. J. Biol. Chem. 285: 14071–14077.

Freund, A., Orjalo, A. V., Desprez, P. –Y. and Campisi, J. 2010. Inflammatory networks during cellular senescence: causes and consequences. Trends in Molecular Medicine. 16: 238–246.

Freund, A., Patil, C. K. and Campisi, J. 2011. p38MAPK is a novel DNA damage response-independent regulator of the senescence-associated secretory phenotype. The EMBO Journal. 30: 1536 – 1548.

Fruman, D. A. and Bismuth, G. 2009. Fine tuning the immune response with PI3K. Immunol. Rev. 228: 253–272.

Fumagalli, M. and d'Adda di Fagagna, F. 2009. SASPense and DDRama in cancer and ageing. Nat. Cell Biol. 11: 921 – 923.

Futami, I., Ishijima, M., Kaneko, H., Tsuji, K., Ichikawa-Tomikawa, N., Sadatsuki, R., Muneta, T., Arikawa-Hirasawa, E., Sekiya, I. and Kaneko, K. 2012. Isolation and Characterization of Multipotential Mesenchymal Cells from the Mouse Synovium. PLoS One. 7: e45517.

Gilbert, L. A. and Hemann, M. T. 2010. DNA Damage-Mediated Induction of a Chemoresistant Niche. Cell. 143: 355-366.

Gilbert, L. A. and Hemann, M. T. 2011. Chemotherapeutic Resistance: Surviving Stressful Situations. Cancer Res. 71: 5062-5066.

Grivennikov, S. I., Greten, F. R., and Karin, M. 2010. Immunity, inflammation, and cancer. Cell. 140: 883–899.

Guertin, D. A. and Sabatini, D. M. 2007. Defining the role of mTOR in cancer. Cancer Cell. 12: 9–22.

Guertin, D. A. and Sabatini, D. M. 2009. The pharmacology of mTOR inhibition. Sci. Signal. 2: pe24.

Hayden, M.S., and Ghosh, S. 2008. Shared Principles in NF-κB Signaling. Cell. 132: 344–362.

Hsieh, A. C., Liu, Y., Edlind, M. P., Ingolia, N. T., Janes, M. R., Sher, A., Shi, E. Y., Stumpf, C. R., Christensen, C., Bonham, M. J., Wang, S., Ren, P., Martin, M., Jessen, K., Feldman, M. E., Weissman, J. S., Shokat, K. M., Rommel, C. and Ruggero, D. 2012. The translational landscape of mTOR signalling steers cancer initiation and metastasis. Nature. 485: 55-61.

Hsu, P. P., Kang, S. A., Rameseder, J., Zhang, Y., Ottina, K. A., Lim, D., et al. 2011. The mTOR-regulated phosphoproteome reveals a mechanism of mTORC1-mediated inhibition of growth factor signaling. Science. 332: 1317–1322.

Janes, M. R. and Fruman, D. A. 2009. Immune regulation by rapamycin: moving beyond T cells. Sci. Signal. 2: pe25.

Janes, M. R., Limon, J. J., So, L., Chen, J., Lim, R. J., Chavez, M. A., Vu, C., Lilly, M. B., Mallya, S., Ong, R. S., Konopleva, M., Martin, M. B., Ren, P., Liu, Y., Rommel, C. and Fruman, D. A. 2010. Effective and selective targeting of leukemia cells using a TORC1/2 kinase inhibitor. Nature Medicine. 16: 205–213.

Jiang, B. and Liu, L. 2008. Role of mTOR in anticancer drug resistance: Perspectives for improved drug treatment. Drug Resistance Updates. 11: 63-76.

Jing, H., Kase, J., Do ¨rr, J. R., Milanovic, M., Lenze, D., Grau, M., Beuster, G., Ji, S., Reimann, M., Lenz, P., et al. 2011. Genes Dev. 25: 2137–2146.

Kapahi P., Chen, D., Rogers, A. N., Katewa, S. D., Li, P. W., Thomas, E. L. and Kockel, L. 2010. With TOR, Less Is More: A Key Role for the Conserved Nutrient-Sensing TOR Pathway in Aging. Cell Metab. 11: 453-465.

Keniry, M. and Parsons, R. 2011. mTOR Inhibition, the Second Generation: ATP-Competitive mTOR Inhibitor Initiates Unexpected Receptor Tyrosine Kinase–Driven Feedback Loop. Cancer Discovery. 1: 203-204.

Kim, J. S., Xu, X., Li, H., Solomon, D., Lane, W. S., Jin, T. and Waldman, T. 2011. Mechanistic Analysis of a DNA Damage-Induced, PTEN-Dependent Size Checkpoint in Human Cells. Mol Cell Biol. 2011. 31: 2756–2771.

Klein, U. and Ghosh, S. 2011. The Two Faces of NF-κB Signaling in Cancer Development and Therapy. Cancer Cell. 20: 556-558.

Kopelovich, L., Fay, J. R., Sigman, C. C. and Crowell, J. A. 2007. The Mammalian Target of Rapamycin Pathway as a Potential Target for Cancer Chemoprevention. Cancer Epidemiol Biomarkers Prev. 16:1330-1340.

Kuilman, T., Michaloglou, C., Mooi, W. J. and Peeper, D. S. 2010. The essence of senescence.

Genes Dev. 2010. 24: 2463-2479.

Kuilman, T., Michaloglou, C., Vredeveld, L. C., Douma, S., van Doorn, R., Desmet, C. J., Aarden, L. A., Mooi, W. J. and Peeper, D. S. 2008. Oncogene-induced senescence relayed by an interleukin-dependent inflammatory network. Cell. 133: 1019–1031.

Kurz, D. J., Decary, S., Hong, Y. and Erusalimsky, J. D.2000. Senescence-associated β-galactosidase reflects an increase in lysosomal mass during replicative ageing of human endothelial cells. Journal of Cell Science. 113: 3613-3622.

Li, H. –F, Kim, J. K. and Waldman, T. 2009. Radiation-induced Akt activation modulates radioresistance in human glioblastoma cells. Radiation Oncology 2009, 4:43.

Liu, M., Lee, D. F., Chen, C. T., Yen, C. J., Li, L. Y., Lee, H. J., et al. 2012. IKKα Activation of NOTCH Links Tumorigenesis via FOXA2 Suppression. Molecular Cell. 45: 171 – 184.

Lu, Y., Azad, N., Wang, L., Iyer, A. K. V., Castranova, V., Jiang, B. and Rojanasakul, Y. 2010. Phosphatidylinositol-3-Kinase/Akt Regulates Bleomycin-Induced Fibroblast Proliferation and Collagen Production. Am J Respir Cell Mol Biol. 42: 432–441.

Manning, B. D. and Cantley, L. C. 2007. AKT/PKB signaling: navigating downstream. Cell. 129: 1261–1274.

Martelli, A. M. et al. 2005. Involvement of the phosphoinositide 3-kinase/Akt signaling pathway in the resistance to therapeutic treatments of human leukemias. Histol. Histopathol. 20: 239–252.

Mickaël Ohanna, Sandy Giuliano, Caroline Bonet, et al. 2011. Senescent cells develop a PARP-1 and nuclear factor-kB-associated secretome (PNAS). Genes Dev. 25: 1245-1261.

Orjalo, A. V., Bhaumik, D., Gengler, B. K., Scott, G. K. and Campisi, J. 2009. Cell surface-bound IL-1α is an upstream regulator of the senescence-associated IL-6/IL-8 cytokine network. Proc Natl Acad Sci U S A. 2009. 106: 17031–17036.

Pasquier, E., Kavallaris, M., and André, N. 2010. Metronomic chemotherapy: new rationale for new directions. Nat Rev Clin Oncol. 7: 455–465.

Pearson, M., Carbone, R., Sebastiani, C., Cioce, M., Fagioli, M., Saito, S., Higashimoto, Y., Appella, E., Minucci, S., Pandolfi, P. P., et al. 2000. PML regulates p53 acetylation and premature senescence induced by oncogenic Ras. Nature. 406: 207–210.

Ramanathan, A and Schreiber, S. L. 2009. Direct control of mitochondrial function by mTOR. Proc Natl Acad Sci U S A. 106: 22229–22232.

Reiling, J. H., and D. M. Sabatini. 2006. Stress and mTORture signaling. Oncogene 25: 6373–6383.

Rodier, F., Coppé, J. -P., Patil, C. K., Hoeijmakers, W. A. M., Muñoz, D. P., Raza, S. R., Freund, A., Campeau, E., Davalos, A. R. and Campisi, J. 2009. Persistent DNA damage signalling triggers senescence-associated inflammatory cytokine secretion. Nature Cell Biology. 11: 973 – 979.

Rodier, F., Muñoz, D. P., Teachenor, R., Chu, V., Le, O., Bhaumik, D., Coppé, J. –P., Campeau, E., Beauséjour, C. M., Kim, S. –H., Davalos, A. R., Campisi, J. 2011. DNA-SCARS: distinct

nuclear structures that sustain damage-induced senescence growth arrest and inflammatory cytokine secretion. J Cell Sci. 124: 68-81.

Roodhart, J. M. L., Daenen, L. G. M., Stigter, E. C. A., Prins, H.- J., Gerrits, J., Houthuijzen, J. M., Gerritsen, M. G., Schipper, H. S., Backer, M. J. G., van Amersfoort. M., et al. 2011. Mesenchymal Stem Cells Induce Resistance to Chemotherapy through the Release of Platinum-Induced Fatty Acids. Cancer Cell. 20: 370-383.

Samuels, Y. and Ericson, K. 2006. Oncogenic PI3K and its role in cancer. Curr. Opin. Oncol. 18: 77–82.

Shah, O. J. and Hunter, T. 2006. Turnover of the active fraction of IRS1 involves raptor-mTOR- and S6K1-dependent serine phosphorylation in cell culture models of tuberous sclerosis. Mol Cell Biol. 26: 6425–6434.

Stanfel MN, Shamieh LS, Kaeberlein M, Kennedy BK. 2009. The TOR pathway comes of age. Biochim Biophys Acta 1790: 1067-1074.

Sung, J. H., Yang, H. -M., Park, J. B., Choi, G. -S., Joh, J. -W., Kwon, C. H., Chun, J. M., Lee, S. -K. and Kim, S. -J. 2008. Isolation and Characterization of Mouse Mesenchymal Stem Cells. Transplantation Proceedings. 40: 2649–2654.

Thomson, A. W., Turnquist, H. R. and Raimondi, G. 2009. Immunoregulatory functions of mTOR inhibition. Nat. Rev. Immunol. 9: 324–337.

Watson, P. A., Ellwood-Yen, K., King, J. C., Wongvipat, J., Lebeau, M. M. and Sawyers, C. L. 2005. Context-dependent hormone-refractory progression revealed through characterization of a novel murine prostate cancer cell line. Cancer Res. 65: 11565-11571.

Wee, S. et al. 2009. PI3K pathway activation mediates resistance to MEK inhibitors in KRAS mutant cancers. Cancer Res. 69:4286–4293.

Wullschleger, S., R. Loewith, and M. N. Hall. 2006. TOR signaling in growth and metabolism. Cell. 124: 471–484.

Yang, H., Rudge, D. G., Koos, J. D., Vaidialingam, B., Yang, H. J. and Pavletich, N. P. 2013. mTOR kinase structure, mechanism and regulation. Nature. 497: 217–223.

Yao, K., Yin, Y. L., Chu, W., Liu, Z., Deng, D., Li, t., Huang, R., Zhang, J., Tan, B., Wang, W. and Wu· G. 2008. Dietary Arginine Supplementation Increases mTOR Signaling Activity in Skeletal Muscle of Neonatal Pigs. J. Nutr. 138: 867-872.

Yu, Y., Yoon, S. O., Poulogiannis, G., Yang, Q., Ma, X. M., Villen, J., et al. 2011. Phosphoproteomic analysis identifies Grb10 as an mTORC1 substrate that negatively regulates insulin signaling. Science. 332: 1322–1326.

Zoncu, R., Efeyan, A. and Sabatini, D. M. 2011 mTOR: from growth signal integration to cancer, diabetes and ageing. Nat Rev Mol Cell Biol. 12: 21–35.

APPENDICES N/A